of p21 mRNA in HEK293 cells transfected with the wild-type p53 expression vector. An increase in ANX4 mRNA was not observed in response to the overexpression of the p53 mutants. Moreover, when LNCaP cells, which endogenously express wild-type p53, were treated with the p53-activating reagent mitomycin C (MMC) or nutlin-3, p21 mRNA and protein levels were elevated along with increase in endogenous p53. Activation of endogenous p53 also increased mRNA and protein levels for ANX4 in LNCaP cells (Fig. 6C, D). These findings support the conclusion that wild-type p53 plays a role in the up-regulation of *ANX4*.

Discussion

The expression of ANX4 is specifically and characteristically enhanced in ovarian CCA cells. This suggests that the expression of *ANX4* is regulated by a molecular mechanism that is unique to these cells. However, the mechanisms for *ANX4* up-regulation in CCA cells have not been elucidated. In the present study, we identified tandem repeats corresponding to the motif for p53 binding in the first intron of the *ANX4* gene, and found (using reporter gene analysis) that this region is a key site for CCA-specific expression. Gene silencing of p53 by siRNA restricted ANX4 transcrip-

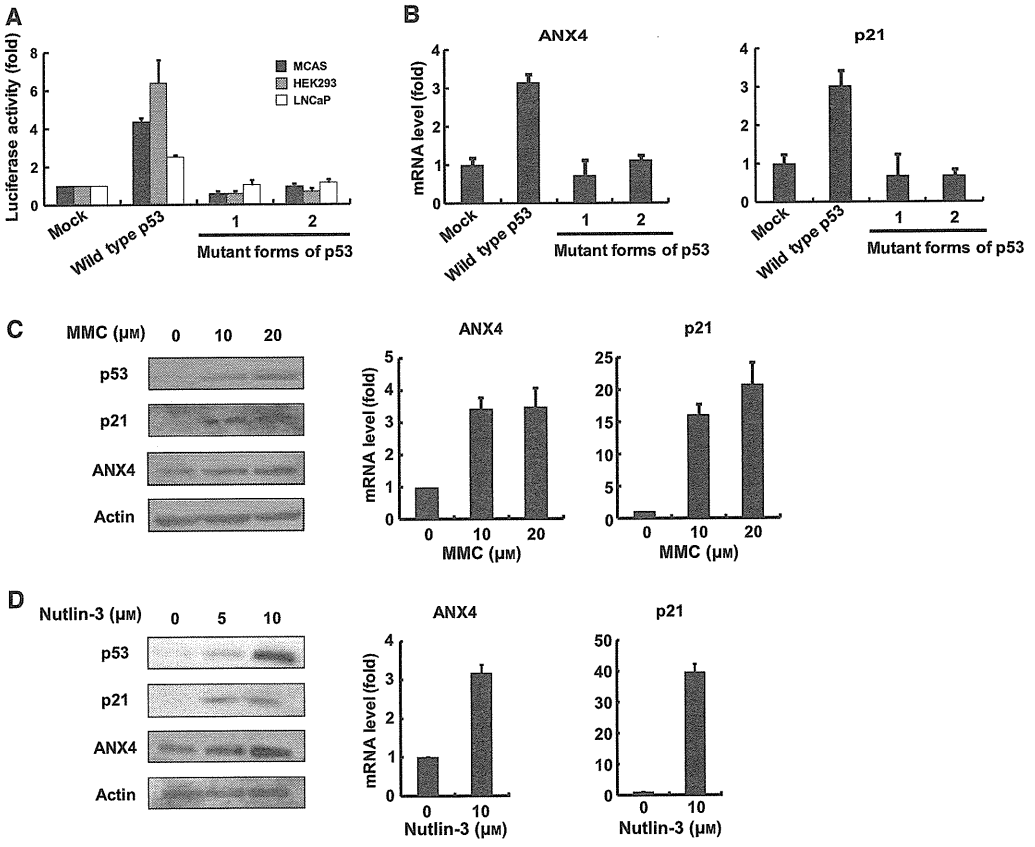

Fig. 6. Wild-type p53 induces *ANX4* gene expression. (A) The overexpression of wild-type p53 enhances the transcriptional activity of the *ANX4*-luciferase reporter. The −43/+541 luc was co-transfected into MCAS, HEK293 and LNCaP with pcDNA3 plasmids encoding the wild-type or mutant forms of p53. Mutant forms 1 and 2 were p53 cDNA cloned from OVCAR-3 and MCAS, respectively. After 48 h, luciferase activity was determined for each sample. The Renilla luciferase reporter vector was co-transfected as an internal control. (B) Overexpression of wild-type p53 activates the expression of ANX4. Wild-type or mutated p53 expression vectors were transfected into HEK293. After 48 h, total RNA was extracted and ANX4 mRNA levels were measured by real-time RT-PCR analyses. (C, D) ANX4 expression increased after p53 activation by MMC or nutlin-3 exposure. LNCaP cells were treated with MMC (C) or nutlin-3 (D). After treatment with MMC for 24 h or nutlin-3 for 12 h at the indicated concentrations, mRNA and protein levels of ANX4 and p21 were measured by western blotting and real-time RT-PCR analyses. The p53 protein levels were also assessed by western blotting to verify that MMC and nutlin-3 activated p53 effectively. The relative mRNA levels were normalized to the level of 18S ribosomal RNA expression in each sample. Actin protein levels were included in the western blotting analysis as a loading control. Bars represent the mean ± SE of three experiments.

tion in CCA cells but not in non-CCA-type EOC cells. No mutations of the *p53* gene were observed in any of the CCA-derived cell lines used in the present study, and p21 and MDM2 transcript levels were relatively higher compared to those in other cell lines in which ANX4 is not abundantly expressed. Moreover, the mRNA levels of ANX4 in other types of cell lines were significantly increased by the overexpression or activation of wild-type p53. Therefore, we conclude that wild-type p53 acts as a positive regulator of ANX4 expression in CCA cells.

The characteristic up-regulation of ANX4 in CCA led us to consider that the protein might be involved in the malignance of CCA by conferring drug resistance or accelerating cancer development. Unexpectedly, we found that the expression of the *ANX4* gene is directly regulated by the tumor suppressor protein p53 in CCA cells. In general, p53 is known to serve as a key player in responding to cellular stresses such as DNA damage, oncogenic activation and microtubule disruption [24,25]. When p53 is activated by such cellular stress, the protein exerts its effect mainly through the transcriptional activation of target genes, including p21, which arrests the cell cycle, and BAX, which induces apoptosis. Thus, p53 typically suppresses cancer development, preventing the division of damaged cells likely to contain mutations and exhibit abnormal cellular growth [26]. Indeed, the *p53* gene is mutated frequently in almost all human cancers [22]. However, among the EOC cell lines used in the present study, *p53* mutations were not observed in any of the CCA-type cell lines, although they were detected in all non-CCA cell lines, which express very low levels of ANX4 (Fig. 5B and Table 1). These findings are in good agreement with studies reporting that *p53* mutations are infrequent in ovarian CCA but occur in at least 50% of the other subtypes of EOC [6–9]. Furthermore, the overexpression of wild-type p53 resulted in an increase in the number of p21 and ANX4 transcripts, whereas overexpressing p53 mutants found in non-CCA cell lines had no effect on the transcription of either gene (Fig. 6). These results show that the p53 mutants in non-CCA cells were inert, compatible with previous findings that *p53* mutations generally result in a loss of wild-type protein activity, dominant-negative activity [27] or an increase in the half-life of the protein by preventing ubiquitination [28]. Therefore, the absence of p53 mutation contributes to the up-regulation of ANX4 in CCA cells. Furthermore, the functional status of p53 was more important. Despite having an intact *p53* gene, HEK293 and LNCaP cell lines expressed trace amounts of ANX4 (Fig. 5). Expression levels of p21 or MDM2 are higher in CCA cell lines than those of HEK293 and LNCaP cell lines, showing a correlation with the expression level of ANX4. Previous immunohistological studies also showed that p21 and MDM2 protein is higher in many ovarian CCA tissues compared to that found in the other EOC subtypes [29,30]. The data obtained in the present study together with those of these previous reports suggest that p53 functional status is critical in governing the ANX4 up-regulation in EOC cells.

Several previous studies have suggested a close relationship between wild-type p53 and *ANX4* expression. ANX4 expression is elevated in renal clear cell carcinoma [31], where *p53* gene mutations are rare [32], and p21 expression has been confirmed by immunohistochemical methods [33]. Moreover, comprehensive expression analysis of p53-induced genes using the p53 temperature-sensitive cell model revealed that ANX4 mRNA was induced after the activation of p53 [34]. ChIP-on-chip analysis using lymphoblastoid cells exposed to ionizing radiation identified 38 kinds of p53-binding genes, and the *ANX4* gene was among the identified genes [35]. These studies strongly support our finding that activated wild-type p53 directly regulates the expression of ANX4 in CCA cells.

In general, p53 has been shown to induce not only genes involved in tumor suppression, such as those that arrest the cell cycle, induce apoptosis and show anti-angiogenic activity, but also oncogenes such as MDM2, p53-inducible protein with RING-H2 domain (*PIRH2*) and constitutively photomorphogenic 1 (*COP1*) [36–38]. These oncogenes are cellular ubiquitin-protein ligases that bind to the p53 protein directly and regulate cellular p53 levels through ubiquitination. The proteasomal degradation of the p53 protein, regulated by a negative feedback mechanism, has been shown to contribute to tumor development. Whether ANX4 should be classified as an oncogene or as a tumor suppressor remains unknown because little is known about its functional role, although ANX4 is reported to be involved in chemoresistance [15,20], activation of chloride ion channels [19], exocytosis [18] and membrane permeability [17]. To clarify the functional and physiological role of the ANX4 protein in ovarian CCA, we are currently conducting proteomic analyses to identify its binding partners.

Because ovarian CCA shows a lower response to the standard paclitaxel–carboplatin combination chemotherapy, a patient with this disease has a worse prognosis than patients with other EOC subtypes, especially serous adenocarcinoma [2]. In CCA, *p53* mutation is infrequently observed [8,9]. Some studies have investigated whether the presence of *p53* mutations correlates with the response to platinum-based

chemotherapy in EOC patients. Lavarino *et al.* [39] and Ueno *et al.* [40] found that, overall, EOCs with wild-type p53 are less responsive to paclitaxel-carboplatin chemotherapy than EOCs with mutated p53 [39,40]. Moreover, when Ueno *et al.* [40] investigated individual EOC subtypes, they observed that this correlation apparently existed in EOC subtypes other than the serous type. Two other interesting studies have reported the suggested involvement of ANX4 in the chemoresistance of human cancer cell lines. Han *et al.* [20] found that the level of ANX4 protein expression was higher in a paclitaxel-resistant cell line derived from a lung cancer cell line than in the parent cell line, and that overexpression of ANX4 cDNA enhanced resistance to paclitaxel in HEK293T cells. Moreover, Kim *et al.* [15] also investigated whether ANX4 was associated with chemoresistance in EOC cell lines, and found that an ANX4-overexpressing cell line derived from the serous-type EOC cell line OVSAHO exhibited greater resistance to carboplatin compared to the parental cell line [15]. Taken together, the findings of these previous studies and our own reveal an association between p53 and ANX4 expression that suggests that tumor cells carrying wild-type p53, such as CCA, may exhibit chemoresistance conferred by p53-dependent ANX4 expression.

In conclusion, analysis of molecular mechanisms underlying CCA-specific ANX4 expression has revealed that the functional status of p53 is involved in the gene regulation in EOC cells. This may lead to a better understanding of the physiological significance of ANX4 up-regulation and the mechanisms underlying malignant progression and chemoresistance in CCA.

Experimental procedures

Cell cultures

Three ovarian cancer cell lines were used for most of the experiments in this study: OVTOKO and OVISE established from ovarian CCA [41], and MCAS, a cell line originating from ovarian mucinous cystadenocarcinoma cloned, as described previously [13]. In some experiments, eight more ovarian cancer cell lines were also used to verify our results. OVKATE, OVSAHO, OVMANA and OVSAYO were established from metastasis ovarian tumors by Yanagibashi *et al.* [42]. OVCAR-3 was obtained from the RIKEN (Tsukuba, Japan) cell bank, and RMUG-S, RMG-I and RMG-II were purchased from the Japanese Collection of Research Bioresources (Tokyo, Japan). RMUG-S, RMG-I and RMG-II were maintained in Ham's F-12 medium, and the other cell lines were cultured in RPMI medium. The human embryonic kidney cell line HEK293 and the prostate adenocarcinoma cell line LNCaP were grown in Ham's F-12 and RPMI 1690 mediums, respectively. All media were supplemented with 10% fetal bovine serum (JRH Biosciences, Inc., Lenexa, KS, USA). Cells were kept at 37 °C in a humidified atmosphere supplemented with 5% CO_2.

Western blotting

Protein was extracted from cells using 30 mM Tris-HCl buffer (pH 7.5) containing 7 M urea, 2 M thiourea, 4% Chaps and 1% dithithreitol. The protein extracts were separated by SDS/PAGE, transferred to poly(vinylidene difluoride) membranes, and blocked by incubation in the reagent Blocking One (Nacalai Tesque, Kyoto, Japan). The blots were then reacted with one of the primary antibodies: goat polyclonal anti-ANX4 (N-19), goat polyclonal anti-actin (I-19), rabbit polyclonal anti-p21 (C-19) and mouse monoclonal anti-MDM2 (SMP-14); all purchased from Santa Cruz Biotechnology (Santa Cruz, CA, USA). Mouse monoclonal anti-ANX4 (No. 50) and anti-p53 (DO-1) were purchased from Funakoshi (Tokyo, Japan) and Calbiochem (San Diego, CA, USA), respectively. Primary antibodies were detected using the ECL Plus Western Blotting Detection System (GE Healthcare, Milwaukee, WI, USA).

Real-time RT-PCR

Total RNA was isolated from the various cell lines using the RNeasy Plus Micro Kit (Qiagen, Hilden, Germany). cDNA was synthesized from the isolated RNA by reverse transcription with the oligo-dT primer and the 18S-rRNA specific primer as described in Zhu and Altmann [43] with one modification, namely, the use of the PrimeScript RT reagent (Takara Bio Inc., Shiga, Japan). Real-time PCR was performed using the Mx3000P Real-Time QPCR System (Agilent Technologies, Santa Clara, CA, USA) with SYBR Premix Ex Taq™ II Perfect Real Time (Takara Bio Inc.). The primer pairs indicated in Table S1 were used for the reactions at a concentration of 10 μM. The PCR products were detected by monitoring the increase in reporter dye fluorescence. mRNA levels were normalized to 18S ribosomal RNA levels.

5′-RACE analysis

Total RNAs isolated from OVTOKO, OVISE and MCAS were reverse-transcribed using the PowerScript reverse transcriptase (Clontech Laboratories, Palo Alto, CA, USA) with the ANX4-RT primer, which is complementary to the nucleotide sequence of the human ANX4 mRNA (GenBank accession number: BC001153). dCTP tails were added to the cDNAs using terminal deoxytransferase (Invitrogen, Carlsbad, CA, USA), and then PCR amplification was per-

formed with the oligo-dI-dG primer and the ANX4-R01 primer (Table S2). The RACE end determined by sequencing analysis was regarded as the transcription start site of *ANX4* and denoted as +1.

Plasmids

For production of luciferase reporter constructs, the flanking region of the transcription start site of *ANX4*, from −1534 to +1010, was amplified from human genomic DNA (Novagen, Darmstadt, Germany) by PCR using KOD-plus DNA polymerase (Toyobo Life Science, Osaka, Japan), and then cloned into the *SmaI*/*BglII* site of pGL3-basic vector (Promega, Madison, WI, USA). The 5′- or 3′-deletion constructs were produced by reacting the amplified PCR products using the primers shown in Table S2 with restriction enzymes. Deletions and mutations in the +180 region were performed by ligating two PCR fragments amplified with a mutation primer, as described previously [44]. To construct the wild-type and mutated p53 expression vectors, full-length p53 cDNAs were isolated from OVISE, OVCAR-3 and MCAS by PCR amplification and then cloned into the *HindIII*/*Eco*RV site of the pcDNA3.1 plasmid (Invitrogen). All constructs were sequenced to verify the orientation and fidelity of the insert.

Luciferase reporter assay

EOC cell lines were seeded on 24-well plates at a density of 2.0×10^5, 3.0×10^5 and 2.5×10^5 cells per well for MCAS, OVTOKO and the other cell lines, respectively. After 24 h, cells were transfected with a pGL3 reporter vector and a pSV-β-galactosidase control vector as an internal control (Promega) using FuGENE HD (Roche, Indianapolis, IN, USA) in accordance with the manufacturer's instructions. For experiments in which p53 was overexpressed, the pRL-TK vector (Promega) was used as an internal control. Then, 42 h after transfection, luciferase activity in cell lysates was measured and normalized to either β-galactosidase activity or Renilla luciferase activity.

ChIP

ChIP assays were performed using the ChIP-IT kit (Active Motif, Carlasbad, CA, USA) in accordance with the manufacturer's instructions. In brief, OVISE, OVTOKO and MCAS cells at 70–80% confluence in 15 cm plates were fixed for 15 min at room temperature with 1% formaldehyde. To shear genomic DNA, the nuclei were subjected to enzymatic digestion with 5 units of enzymatic shearing mixture solution (Active Motif) for 15 min at 37 °C. Sheared chromatin was immunoprecipitated with 4 μg of anti-p53 (DO-1; Calbiochem) or control IgG (Active Motif). Cross-linking was reversed and purified DNA was subjected to PCR. The PCR products were analyzed by electrophoresis on a 2% agarose gel stained with ethidium bromide. Primers employed were designed to detect the predicted p53 binding sites on *ANX4* and *p21* genes. The primer sequences are indicated in Table S3.

Gene silencing of p53

Stealth™ siRNAs (Invitrogen) were used to silence the *p53* gene. Two kinds of Stealth™ siRNAs were tested for their RNA interference (RNAi) activity against the *p53* gene, and the one resulting in a higher level of knockdown was selected for further use. The targeted sequence of the selected siRNA was 5′-UGGAAGACUCCAGUGGUAAUCUACU-3′, corresponding to nucleotides 890–914 of the p53 mRNA (GenBank accession number: BC003596). Control experiments used the Stealth™ RNAi negative control MED (Invitrogen). EOC cells were transfected with the Stealth™ siRNAs using Lipofectamine RNAi MAX (Invitrogen) in accordance with the manufacturer's instructions. For the luciferase assay, siRNA-transfected cells were incubated for 24 h in one well of a 24-well plate, and then transfected with reporter vectors. For western blotting or real-time RT-PCR analyses, all cell lines were transfected with siRNA and grown for 72 h.

p53 mutation analysis

The p53 cDNAs from various cell lines were amplified by PCR using the KOD-plus DNA polymerase (Toyobo Life Science) and *p53*-specific primers (sense 5′-CACGACGGT GACACGCTTCC-3′ and antisense 5′-CCTGGGTGCTT CTGACGCAC-3′) corresponding to nucleotides 64–83 and 1404–1423 of the p53 mRNA, respectively (GenBank accession number: BC003596). The PCR products were purified using the Wizard SV Gel and the PCR Clean-Up System (Promega) and then subjected to sequence analyses.

p53 activation by drug treatment

LNCaP cells were grown to 60–70% confluency in six-well plates, and then treated with different concentrations of MMC (Calbiochem) for 24 h, or nutlin-3 (Cayman Chemical, Ann Arbor, MI, USA) for 12 h. After treatment, cells were subjected to real-time RT-PCR and western blotting.

Acknowledgements

This work was supported in part by a Grant-in-Aid for young Scientists (B) 18790226 and 20790262 from The Ministry of Education, Culture, Sports, Science and Technology, Japan. We thank Dr Youhei Miyagi (Kanagawa Cancer Center, Kanagawa, Japan) and Dr Masato Katsuyama (Kyoto Prefectural University of Medicine, Kyoto, Japan) for insightful discussions.

References

1 Bray F, Loos AH, Tognazzo S & La Vecchia C (2005) Ovarian cancer in Europe: cross-sectional trends in incidence and mortality in 28 countries, 1953-2000. *Int J Cancer* **113**, 977–990.

2 Sugiyama T, Kamura T, Kigawa J, Terakawa N, Kikuchi Y, Kita T, Suzuki M, Sato I & Taguchi K (2000) Clinical characteristics of clear cell carcinoma of the ovary: a distinct histologic type with poor prognosis and resistance to platinum-based chemotherapy. *Cancer* **88**, 2584–2589.

3 Itamochi H, Kigawa J, Akeshima R, Sato S, Kamazawa S, Takahashi M, Kanamori Y, Suzuki M, Ohwada M & Terakawa N (2002) Mechanisms of cisplatin resistance in clear cell carcinoma of the ovary. *Oncology* **62**, 349–353.

4 Itamochi H, Kigawa J, Sugiyama T, Kikuchi Y, Suzuki M & Terakawa N (2002) Low proliferation activity may be associated with chemoresistance in clear cell carcinoma of the ovary. *Obstet Gynecol* **100**, 281–287.

5 Itamochi H, Kigawa J & Terakawa N (2008) Mechanisms of chemoresistance and poor prognosis in ovarian clear cell carcinoma. *Cancer Sci* **99**, 653–658.

6 Marks JR, Davidoff AM, Kerns BJ, Humphrey PA, Pence JC, Dodge RK, Clarke-Pearson DL, Iglehart JD, Bast RC Jr & Berchuck A (1991) Overexpression and mutation of p53 in epithelial ovarian cancer. *Cancer Res* **51**, 2979–2984.

7 Kohler MF, Marks JR, Wiseman RW, Jacobs IJ, Davidoff AM, Clarke-Pearson DL, Soper JT, Bast RC Jr & Berchuck A (1993) Spectrum of mutation and frequency of allelic deletion of the p53 gene in ovarian cancer. *J Natl Cancer Inst* **85**, 1513–1519.

8 Ho ES, Lai CR, Hsieh YT, Chen JT, Lin AJ, Hung MH & Liu FS (2001) p53 mutation is infrequent in clear cell carcinoma of the ovary. *Gynecol Oncol* **80**, 189–193.

9 Okuda T, Otsuka J, Sekizawa A, Saito H, Makino R, Kushima M, Farina A, Kuwano Y & Okai T (2003) p53 mutations and overexpression affect prognosis of ovarian endometrioid cancer but not clear cell cancer. *Gynecol Oncol* **88**, 318–325.

10 Saegusa M, Machida BD & Okayasu I (2001) Possible associations among expression of p14(ARF), p16(INK4a), p21(WAF1/CIP1), p27(KIP1), and p53 accumulation and the balance of apoptosis and cell proliferation in ovarian carcinomas. *Cancer* **92**, 1177–1189.

11 Schaner ME, Ross DT, Ciaravino G, Sorlie T, Troyanskaya O, Diehn M, Wang YC, Duran GE, Sikic TL, Caldeira S *et al.* (2003) Gene expression patterns in ovarian carcinomas. *Mol Biol Cell* **14**, 4376–4386.

12 Schwartz DR, Kardia SL, Shedden KA, Kuick R, Michailidis G, Taylor JM, Misek DE, Wu R, Zhai Y, Darrah DM *et al.* (2002) Gene expression in ovarian cancer reflects both morphology and biological behavior, distinguishing clear cell from other poor-prognosis ovarian carcinomas. *Cancer Res* **62**, 4722–4729.

13 Morita A, Miyagi E, Yasumitsu H, Kawasaki H, Hirano H & Hirahara F (2006) Proteomic search for potential diagnostic markers and therapeutic targets for ovarian clear cell adenocarcinoma. *Proteomics* **6**, 5880–5890.

14 Zhu Y, Wu R, Sangha N, Yoo C, Cho KR, Shedden KA, Katabuchi H & Lubman DM (2006) Classifications of ovarian cancer tissues by proteomic patterns. *Proteomics* **6**, 5846–5856.

15 Kim A, Enomoto T, Serada S, Ueda Y, Takahashi T, Ripley B, Miyatake T, Fujita M, Lee CM, Morimoto K *et al.* (2009) Enhanced expression of annexin A4 in clear cell carcinoma of the ovary and its association with chemoresistance to carboplatin. *Int J Cancer* **125**, 2316–2322.

16 Moss SE & Morgan RO (2004) The annexins. *Genome Biol* **5**, 219.

17 Hill WG, Kaetzel MA, Kishore BK, Dedman JR & Zeidel ML (2003) Annexin A4 reduces water and proton permeability of model membranes but does not alter aquaporin 2-mediated water transport in isolated endosomes. *J Gen Physiol* **121**, 413–425.

18 Sohma H, Creutz CE, Gasa S, Ohkawa H, Akino T & Kuroki Y (2001) Differential lipid specificities of the repeated domains of annexin IV. *Biochim Biophys Acta* **1546**, 205–215.

19 Xie W, Kaetzel MA, Bruzik KS, Dedman JR, Shears SB & Nelson DJ (1996) Inositol 3,4,5,6-tetrakisphosphate inhibits the calmodulin-dependent protein kinase II-activated chloride conductance in T84 colonic epithelial cells. *J Biol Chem* **271**, 14092–14097.

20 Han EK, Tahir SK, Cherian SP, Collins N & Ng SC (2000) Modulation of paclitaxel resistance by annexin IV in human cancer cell lines. *Br J Cancer* **83**, 83–88.

21 el-Deiry WS, Kern SE, Pietenpol JA, Kinzler KW & Vogelstein B (1992) Definition of a consensus binding site for p53. *Nat Genet* **1**, 45–49.

22 Levine AJ, Momand J & Finlay CA (1991) The p53 tumour suppressor gene. *Nature* **351**, 453–456.

23 Bourdon JC, Fernandes K, Murray-Zmijewski F, Liu G, Diot A, Xirodimas DP, Saville MK & Lane DP (2005) p53 isoforms can regulate p53 transcriptional activity. *Genes Dev* **19**, 2122–2137.

24 Meek DW (1998) Multisite phosphorylation and the integration of stress signals at p53. *Cell Signal* **10**, 159–166.

25 Lane DP (1992) Cancer. p53, guardian of the genome. *Nature* **358**, 15–16.

26 Ryan KM, Phillips AC & Vousden KH (2001) Regulation and function of the p53 tumor suppressor protein. *Curr Opin Cell Biol* **13**, 332–337.

27 Levesque MA, Katsaros D, Yu H, Zola P, Sismondi P, Giardina G & Diamandis EP (1995) Mutant p53 protein overexpression is associated with poor outcome in patients with well or moderately differentiated ovarian carcinoma. *Cancer* **75**, 1327–1338.
28 Eltabbakh GH, Belinson JL, Kennedy AW, Biscotti CV, Casey G, Tubbs RR & Blumenson LE (1997) p53 overexpression is not an independent prognostic factor for patients with primary ovarian epithelial cancer. *Cancer* **80**, 892–898.
29 Shimizu M, Nikaido T, Toki T, Shiozawa T & Fujii S (1999) Clear cell carcinoma has an expression pattern of cell cycle regulatory molecules that is unique among ovarian adenocarcinomas. *Cancer* **85**, 669–677.
30 Skomedal H, Kristensen GB, Abeler VM, Borresen-Dale AL, Trope C & Holm R (1997) TP53 protein accumulation and gene mutation in relation to overexpression of MDM2 protein in ovarian borderline tumours and stage I carcinomas. *J Pathol* **181**, 158–165.
31 Zimmermann U, Balabanov S, Giebel J, Teller S, Junker H, Schmoll D, Protzel C, Scharf C, Kleist B & Walther R (2004) Increased expression and altered location of annexin IV in renal clear cell carcinoma: a possible role in tumour dissemination. *Cancer Lett* **209**, 111–118.
32 Hsueh C, Wang H, Gonzalez-Crussi F, Lin JN, Hung IJ, Yang CP & Jiang TH (2002) Infrequent p53 gene mutations and lack of p53 protein expression in clear cell sarcoma of the kidney: immunohistochemical study and mutation analysis of p53 in renal tumors of unfavorable prognosis. *Mod Pathol* **15**, 606–610.
33 Weiss RH, Borowsky AD, Seligson D, Lin PY, Dillard-Telm L, Belldegrun AS, Figlin RA & Pantuck AD (2007) p21 is a prognostic marker for renal cell carcinoma: implications for novel therapeutic approaches. *J Urol* **177**, 63–68.
34 Robinson M, Jiang P, Cui J, Li J, Wang Y, Swaroop M, Madore S, Lawrence TS & Sun Y (2003) Global genechip profiling to identify genes responsive to p53-induced growth arrest and apoptosis in human lung carcinoma cells. *Cancer Biol Ther* **2**, 406–415.
35 Jen KY & Cheung VG (2005) Identification of novel p53 target genes in ionizing radiation response. *Cancer Res* **65**, 7666–7673.
36 Li M, Brooks CL, Wu-Baer F, Chen D, Baer R & Gu W (2003) Mono- versus polyubiquitination: differential control of p53 fate by Mdm2. *Science* **302**, 1972–1975.
37 Leng RP, Lin Y, Ma W, Wu H, Lemmers B, Chung S, Parant JM, Lozano G, Hakem R & Benchimol S (2003) Pirh2, a p53-induced ubiquitin-protein ligase, promotes p53 degradation. *Cell* **112**, 779–791.
38 Dornan D, Wertz I, Shimizu H, Arnott D, Frantz GD, Dowd P, O'Rourke K, Koeppen H & Dixit VM (2004) The ubiquitin ligase COP1 is a critical negative regulator of p53. *Nature* **429**, 86–92.
39 Lavarino C, Pilotti S, Oggionni M, Gatti L, Perego P, Bresciani G, Pierotti MA, Scambia G, Ferrandina G, Fagotti A *et al.* (2000) p53 gene status and response to platinum/paclitaxel-based chemotherapy in advanced ovarian carcinoma. *J Clin Oncol* **18**, 3936–3945.
40 Ueno Y, Enomoto T, Otsuki Y, Sugita N, Nakashima R, Yoshino K, Kuragaki C, Ueda Y, Aki T, Ikegami H *et al.* (2006) Prognostic significance of p53 mutation in suboptimally resected advanced ovarian carcinoma treated with the combination chemotherapy of paclitaxel and carboplatin. *Cancer Lett* **241**, 289–300.
41 Gorai I, Nakazawa T, Miyagi E, Hirahara F, Nagashima Y & Minaguchi H (1995) Establishment and characterization of two human ovarian clear cell adenocarcinoma lines from metastatic lesions with different properties. *Gynecol Oncol* **57**, 33–46.
42 Yanagibashi T, Gorai I, Nakazawa T, Miyagi E, Hirahara F, Kitamura H & Minaguchi H (1997) Complexity of expression of the intermediate filaments of six new human ovarian carcinoma cell lines: new expression of cytokeratin 20. *Br J Cancer* **76**, 829–835.
43 Zhu LJ & Altmann SW (2005) mRNA and 18S-RNA coapplication-reverse transcription for quantitative gene expression analysis. *Anal Biochem* **345**, 102–109.
44 Kato Y, Arakawa N, Masuishi Y, Kawasaki H & Hirano H (2009) Mutagenesis of longer inserts by the ligation of two PCR fragments amplified with a mutation primer. *J Biosci Bioeng* **107**, 95–97.

Supporting information

The following supplementary material is available:
Fig. S1. The +180 region is essential for CCA-specific transcriptional activity of *ANX4*.
Table S1. Nucleotide sequences of the primers used in real-time RT-PCR.
Table S2. Nucleotide sequences of the primers used for 5′-RACE and plasmid construction.
Table S3. Nucleotide sequences of the primers used in the ChIP assay.

This supplementary material can be found in the online version of this article.

Please note: As a service to our authors and readers, this journal provides supporting information supplied by the authors. Such materials are peer-reviewed and may be re-organized for online delivery, but are not copy-edited or typeset. Technical support issues arising from supporting information (other than missing files) should be addressed to the authors.

THE JOURNAL OF BIOLOGICAL CHEMISTRY VOL. 286, NO. 13, pp. 11593–11603, April 1, 2011

A Distinct Role for Pin1 in the Induction and Maintenance of Pluripotency*

Received for publication, September 23, 2010, and in revised form, February 3, 2011 Published, JBC Papers in Press, February 4, 2011, DOI 10.1074/jbc.M110.187989

Mayuko Nishi,[a] Hidenori Akutsu,[b] Shinji Masui,[c] Asami Kondo,[a] Yoji Nagashima,[d] Hirokazu Kimura,[e] Kilian Perrem,[f] Yasushi Shigeri,[g] Masashi Toyoda,[b] Akiko Okayama,[h] Hisashi Hirano,[h] Akihiro Umezawa,[b] Naoki Yamamoto,[i] Sam W. Lee,[j] and Akihide Ryo[a1]

From the Departments of [a]Microbiology, [d]Pathology, and [h]Supramolecular Biology, Yokohama City University School of Medicine, Yokohama 236-0004, Japan, the [b]Department of Reproductive Biology, National Research Institute for Child Health and Development, Tokyo 157-8535, Japan, the [c]Department of Regenerative Medicine, Research Institute, International Medical Center of Japan, Tokyo 162-8655, Japan, the [e]Infectious Disease Surveillance Center, National Institute of Infectious Diseases, Tokyo 208-0011, Japan, the [f]Commonwealth Scientific and Industrial Research Organization, P.O. Box 225, Dickson, Australian Capital Territory 2602, Australia, the [g]National Institute of Advanced Industrial Science and Technology, Osaka 563-8577, Japan, the [i]Department of Microbiology, National University of Singapore, 117597 Singapore, and the [j]Cutaneous Biology Research Center, Massachusetts General Hospital and Harvard Medical School, Charlestown, Massachusetts 02129

The prominent characteristics of pluripotent stem cells are their unique capacity to self-renew and pluripotency. Although pluripotent stem cell proliferation is maintained by specific intracellular phosphorylation signaling events, it has not been well characterized how the resulting phosphorylated proteins are subsequently regulated. We here report that the peptidyl-prolyl isomerase Pin1 is indispensable for the self-renewal and maintenance of pluripotent stem cells via the regulation of phosphorylated Oct4 and other substrates. Pin1 expression was found to be up-regulated upon the induction of induced pluripotent stem (iPS) cells, and the forced expression of Pin1 with defined reprogramming factors was observed to further enhance the frequency of iPS cell generation. The inhibition of Pin1 activity significantly suppressed colony formation and induced the aberrant differentiation of human iPS cells as well as murine ES cells. We further found that Pin1 interacts with the phosphorylated Ser^{12}-Pro motif of Oct4 and that this in turn facilitates the stability and transcriptional activity functions of Oct4. Our current findings thus uncover an atypical role for Pin1 as a putative regulator of the induction and maintenance of pluripotency via the control of phosphorylation signaling. These data suggest that the manipulation of Pin1 function could be a potential strategy for the stable induction and proliferation of human iPS cells.

Stem cells are characterized by their ability to self-renew through mitotic cell division and to differentiate into a diverse range of specialized cell types (1, 2). Human pluripotent stem cell proliferation is maintained through the action of several transcription factors including Oct4 (octamer 4), SOX2, Klf-4, Nanog, and c-Myc, which perform reprogramming functions under the stimulatory effects of stem cell-specific growth factors, including basic fibroblast growth factor (3–5). Basic fibroblast growth factor signaling has been shown to be essential for pluripotency as its depletion from cell culture media leads to aberrant cell differentiation and cell death (6, 7). Fibroblast growth factors produce mitogenic effects in targeted cells via signaling through cell surface receptor tyrosine kinases (8). These kinases can initiate intracellular signaling in cells, which is transmitted and diffused by tyrosine phosphorylation of the assembled proteins and of cellular substrates, including protein kinases with specificity for serine/threonine residues (8, 9). Although this intracellular phosphorylation signaling might indeed contribute to the self-renewal and pluripotency of stem cells (10, 11), it has not yet been fully determined how these phosphorylated proteins are further regulated.

Protein phosphorylation is a fundamental mode of intracellular signal transduction in a variety of key cellular processes such as cell proliferation, differentiation, and morphogenesis (12). A pivotal signaling mechanism that controls the function of phosphorylated proteins is the *cis-trans* isomerization of phosphorylated Ser/Thr-Pro motifs by the peptidylprolyl isomerase Pin1 (13, 14). This modification regulates multiple intracellular signaling pathways, including ErbB2/Ras, Wnt/β-catenin, and NF-κB, and thus plays an important role in the etiology of several human diseases (15–18). These include various cancers, Alzheimer disease, and immune disorders (14, 17, 18). However, the role of Pin1 in regulating the properties of pluripotent stem cells has not been adequately investigated to date.

In our current study, we investigated the role of Pin1 in the self-renewal and stemness of pluripotent stem cells. We reveal that Pin1 is induced upon cellular reprogramming and that its blockade significantly inhibits the self-renewal and maintenance of human iPS[2] cells in addition to murine ES cells. We find also that Pin1 can interact with phosphorylated Oct4 at the

* This work was supported in part by grants from the Takeda Science Foundation, Uehara Memorial Foundation, and Kanagawa Nanbyo Foundation (to A. R.).

[1] To whom correspondence should be addressed: Dept. of Microbiology, Yokohama City University School of Medicine, 3-9 Fuku-ura, Kanazawa-ku, Yokohama 236-0004, Japan. Tel.: 81-45-787-2602; Fax: 81-45-787-2851; E-mail: aryo@yokohama-cu.ac.jp.

[2] The abbreviations used are: iPS, induced pluripotent stem; AP, alkaline phosphatase; dnPin1, dominant-negative Pin1; 4F, four reprogramming factors; DMSO, dimethyl sulfoxide; SUMO, small ubiquitin-like modifier; Oct4, Octamer 4.

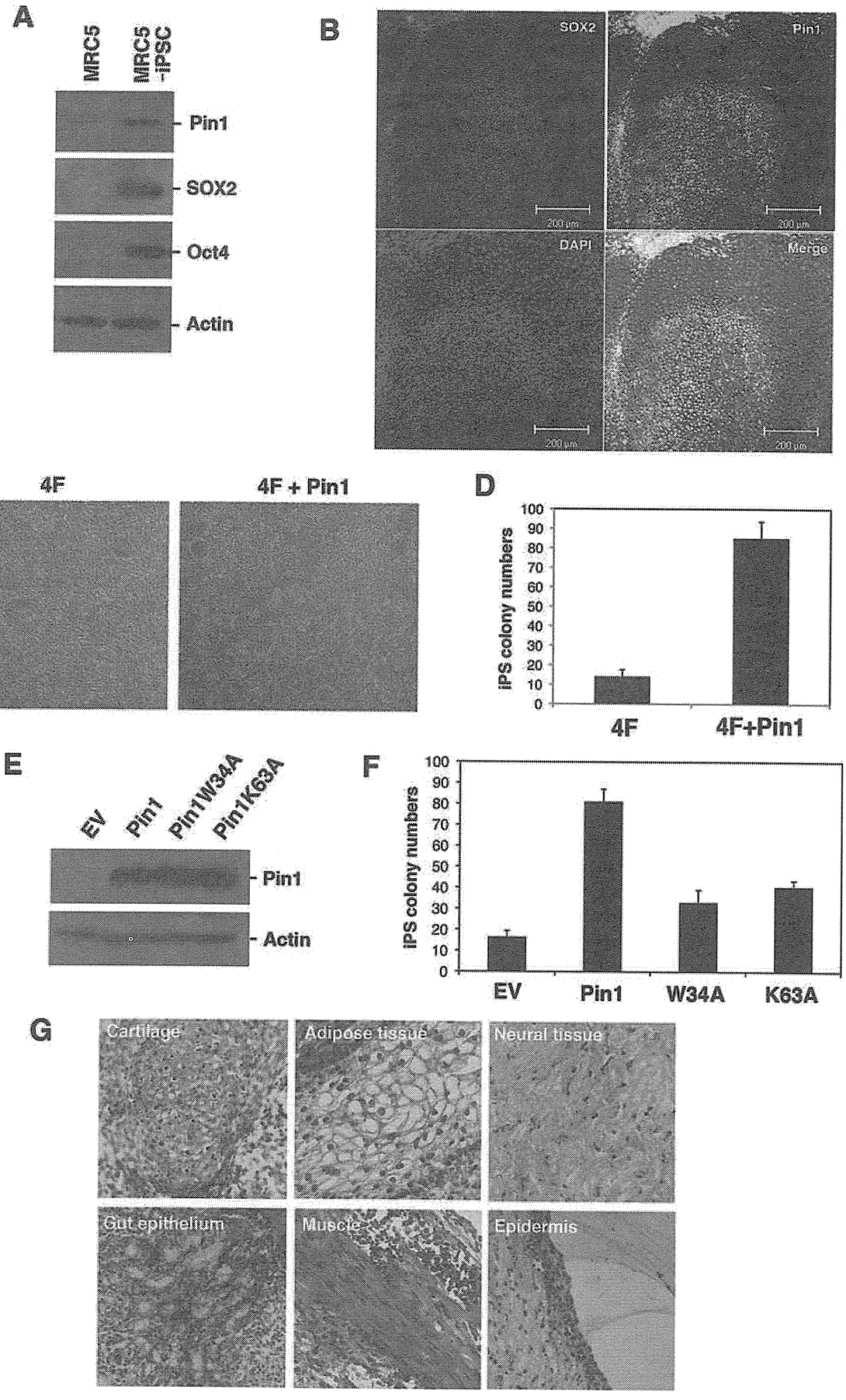

Ser[12]-Pro motif in this protein. This enhances the stability and hence the transcriptional activity of Oct4. Our present data thus suggest that Pin1 is indeed a putative regulator of the self-renewal and proliferation of pluripotent stem cells.

EXPERIMENTAL PROCEDURES

Colony Formation Analysis—Human iPS cells were obtained from the RIKEN BioResource Center (clone no. 201B7) (19). Cells were cultured in human embryonic stem cell culture medium (KnockOut Dulbecco's modified Eagle's medium (Invitrogen)) supplemented with 20% KnockOut SR (Invitrogen), 1% GlutaMAX (Invitrogen), 100 μM nonessential amino acids (Invitrogen), 50 μM β-mercaptoethanol, and 10 ng/ml basic fibroblast growth factor). Murine ES cells were cultured in human embryonic stem cell culture medium (KnockOut Dulbecco's modified Eagle's medium supplemented with 15% KnockOut SR, 1% GlutaMAX (Invitrogen), 100 μM nonessential amino acids, 50 μM β-mercaptoethanol, and 1000 units/ml recombinant human leukemia inhibitory factor) (20). Colony formation was scored by counting the number of alkaline phosphatase (AP)-positive colonies as described previously (21). The number of cells per colony was determined by manually counting the number of DAPI-stained cells (21).

Cell Reprogramming—MRC5 fibroblasts were transduced with retroviral vectors encoding reprogramming factors as described previously (19). Briefly, the retroviral vector plasmids pMXs-hOct4, pMXs-hSOX2, pMXs-hKLF4, pMXs-hcMYC (Addgene), and pVSV-G were introduced into Plat-E cells using Effectene transfection reagent (Qiagen). After 48 h, virus-containing supernatants were passed through a 0.45-μm filter and supplemented with 10 μg/ml hexadimethrine bromide (polybrene). Cells were seeded at 6×10^5 cells per 60 mm dish at 24 h before incubation in the virus/polybrene-containing supernatants for 16 h. After 6 days, cells were plated on irradiated mouse embryonic fibroblasts, and culture medium was replaced with the hESC culture medium 24 h later. Cells were maintained at 37 °C and 5% CO_2 for 30 days.

Construction of Expression Vectors—Oct4 cDNA was subcloned into pcDNA3-HA expression vector (Invitrogen). Expression constructs of Oct4 were as follows: pcDNA-HA-Oct4 wild-type, amino acids 1–360; pcDNA-HA-Oct4 ΔC, amino acids 1–297; pcDNA-HA-Oct4 ΔN1, amino acids 138–360; pcDNA-HA-Oct4 ΔN2, amino acids 113–360; and pcDNA-HA-Oct4 ΔN3, amino acids 34–360. pcDNA-HA-Oct4-S12A was generated by KOD-Plus Mutagenesis Kit (Toyobo, Osaka, Japan) according to the manufacturer's instructions. The primers were 5′-CGCCCCCTCCAGGTGGT-3′ (forward) and 5′-CGAAGGCAAAATCTGAAGCC-3′ (reverse).

Gene Reporter Assay—A pGL3-fgf4 reporter plasmid containing an Oct-SOX binding cassette and the firefly luciferase gene was transfected with pRL-CMV (22). The −2601/+1 (nucleotide positions indicated with respect to the +1 translation start site) genomic fragment of the Oct4 promoter upstream region was amplified by PCR from human lymphocyte genomic DNA and cloned into the KpnI/HindIII sites of the pGL4-basic reporter plasmid (Promega, Madison, WI) as described previously (23). The primer sets were as follows: 5′-CCTGGTACCAGGATGGCAAGCTGAGAAACACTG-3′ and 5′-TCGCAAGCTTGCGAAGGGACTACTCAAC-3′. Cells were transfected with reporter plasmid vectors using Effectene (Qiagen) or Xfect Stem (Clontech). One day after transfection, the cells were resuspended in passive lysis buffer (Promega) and incubated for 15 min at room temperature. Luciferase activities were measured with a Dual-Luciferase reporter assay system (Promega) in accordance with the manufacturer's instructions.

GST Pulldown Assay and Immunoprecipitation Analysis—Cells were lysed with GST pulldown buffer (50 mM HEPES (pH 7.4), 150 mM NaCl, 10% glycerol, 1% Triton X-100, 1.5 mM $MgCl_2$, 1 mM EGTA, 100 mM NaF, 1 mM Na_3VO_4, 1 mM DTT, 5 μg/ml leupeptin, 1 μg/ml pepstatin, and 0.2 mM PMSF) and incubated with 30 μl of glutathione-agarose beads containing either GST-Pin1 or GST at 4 °C for 2 h. The precipitated proteins were then washed three times with lysis buffer and subjected to SDS-PAGE. For immunoprecipitation, cells were lysed with Nonidet P-40 lysis buffer (10 mM Tris HCl (pH 7.4), 100 mM NaCl, 0.5% Nonidet P-40, 1 mM Na_3VO_4, 100 mM NaF, 5 μg/ml leupeptin, 1 μg/ml pepstatin, and 0.2 mM PMSF). Cell lysates were incubated for 1 h with protein A/G-Sepharose·nonimmunized IgG complexes. Supernatant fractions were recovered and immunoprecipitated with 5 μg of anti-Myc antibody and 30 μl protein A/G-Sepharose. After washing three times with lysis buffer, the pellets were analyzed by SDS-PAGE.

Proteomics Analysis—Human iPS cell lysates were processed for immunoprecipitation with a monoclonal anti-Pin1 antibody (clone 257417, R&D Systems) at 4 °C for 3 h followed by SDS-PAGE. Gel lanes corresponding to the region from ~30 to 150 kDa were systematically excised, and the pieces were reduced, alkylated, and trypsinized. Peptides were analyzed by the linear ion trap Orbitrap hybrid mass spectrometer (Thermo Scientific). Protein identification was performed by peptide

FIGURE 1. **Pin1 is preferentially expressed in human iPS cells.** *A*, immunoblotting analysis of Oct4, SOX2, and Pin1 in MRC5 and MRC5-derived iPS cells. Actin was used as a loading control. *iPSC*, induced pluripotent stem cells; *EV*, empty vector. *B*, immunofluorescent analysis of Pin1 and SOX2 in human iPS cells. Representative images of phase-contrast microscopy and fluorescent immunocytochemistry for SOX2 (*red*) and Pin1 (*green*) are shown. Nuclei are indicated by DAPI staining (*blue*). Note that Pin1 is highly expressed in SOX2-positive pluripotent stem cells. *C* and *D*, Pin1 expression enhances 4F (Oct4, SOX2, Klf4, and c-Myc)-induced iPS cell induction. MRC5 fibroblasts were infected with retrovirus vectors encoding 4F and co-infected with those encoding either empty vector or Pin1. A representative picture of colony formations stained with AP is shown (*C*). The numbers of AP-positive colonies were scored in three independent experiments (*D*). Note that the co-introduction of Pin1 with 4F increases the frequency of iPS colony formation. *E* and *F*, MRC5 fibroblasts were infected with retrovirus vectors encoding 4F and co-infected with those encoding empty vector, HA-tagged wild-type Pin1, or its W34A or K63A mutants. The expression levels of HA-Pin1 or its mutants in infected MRC5 cells were analyzed by immunoblotting analysis with anti-HA antibody (*E*). The number of AP-positive colonies was scored in three independent experiments (*F*). *G*, teratoma tissue derived from human iPS cells induced by 4F and Pin1. iPS cells were transplanted subcutaneously into immunodeficient mice (2×10^6/mouse). Representative images of hematoxylin and eosin stained tumor with light microscope (200×) are shown.

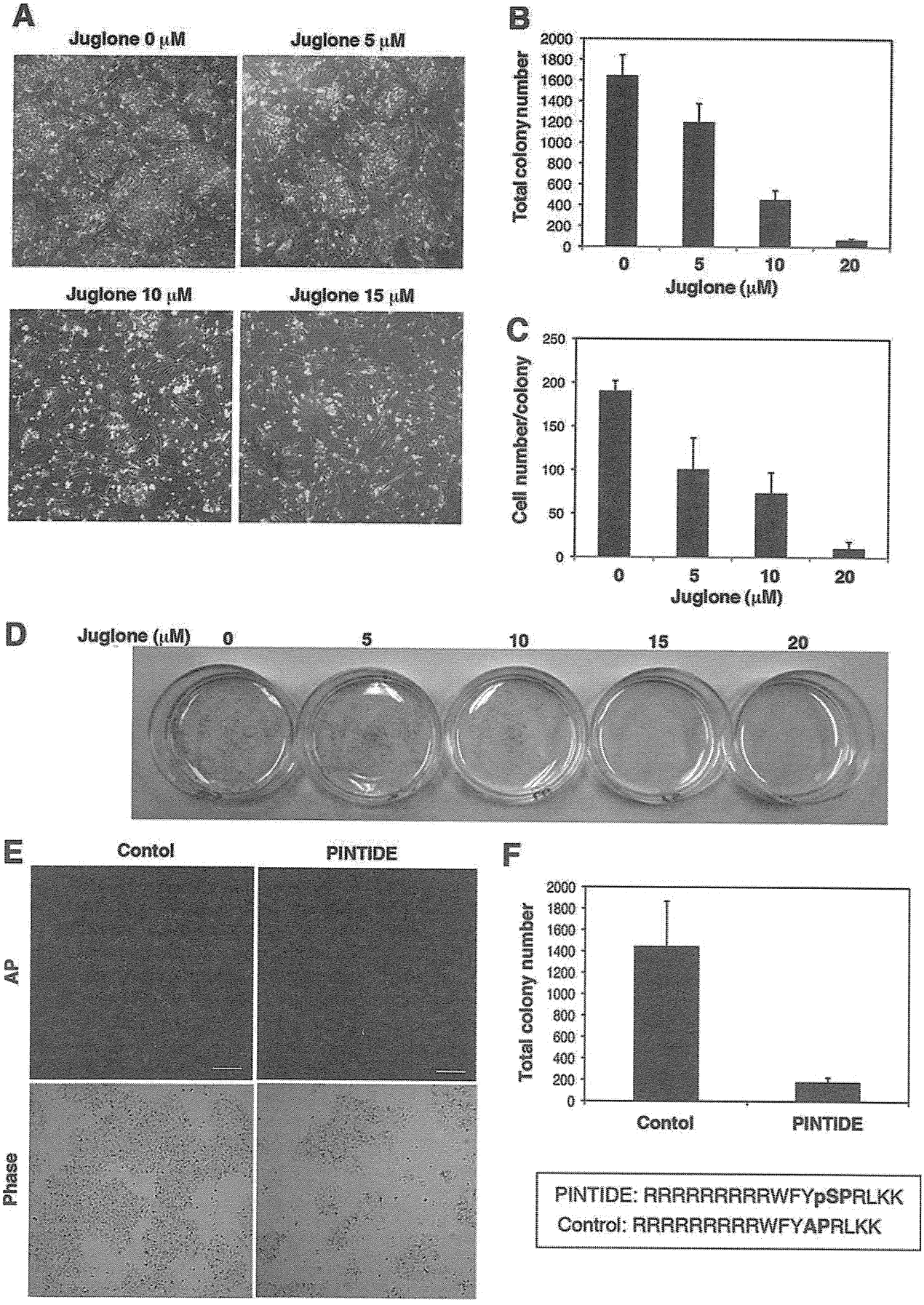

mass fingerprinting with the Mascot and Aldente search algorithms.

Quantitative Real-time PCR—Total RNA was extracted with TRIzol reagent (Invitrogen) according to the manufacturer's protocol. cDNA was synthesized using a cDNA synthesis kit (Toyobo, Osaka, Japan) and subjected to RT-PCR analysis with the SYBR Premix Ex gent Kit TaqII (Takara Bio, Shiga, Japan) using an Applied Biosystems 7300 real-time PCR System. The primer sets used were as follows: mOct4, 5′-CGTGTGAGGTGGAGTCTGGAGACC-3′ and 5′-ACTCGAACCACATCCTTCTCTAGCC-3′; mGAPDH, 5′-CCATGGAGAAGGCTGGGG-3′ and 5′-CAAAGTTGTCATGGATGACC-3′.

Teratoma Formation—Cells were harvested using accutase, collected into tubes, and centrifuged. The pellets were then suspended in human ESC culture medium. Fox Chase severe combined immunodeficiency mice (CREA, Tokyo, Japan) were injected with 2×10^6 cells mixed with an equal volume of Matrigel (BD Biosciences). Frozen tumor tissues embedded in optimum cutting temperature compound were sliced by cryosectioning and stained with hematoxylin and eosin.

RESULTS

Pin1 Is Induced upon Cellular Reprogramming and Enhances Generation of iPS Cells—To examine the role of Pin1 in cellular reprogramming and pluripotency, we initially investigated the expression levels of this prolyl isomerase in human iPS cells. Pin1 was found to be significantly induced upon the generation of iPS cells derived from MRC5 human fibroblasts (Fig. 1*A*). Immunofluorescent analysis further revealed that Pin1 is selectively expressed in SOX2-positive pluripotent stem cells, whereas its expression was found to be significantly suppressed in the surrounding SOX2-negative differentiated cells (Fig. 1*B*). These results indicate that Pin1 is preferentially expressed in reprogramming stem cells.

We next evaluated whether Pin1 affects the reprogramming of somatic cells into iPS cells. The co-infection of a Pin1-encoding retrovirus vector with those encoding four defined reprogramming factors (4F; SOX2, Oct4, Klf-4, and c-Myc) (24) notably boosted the generation of AP-positive iPS cell colonies compared with an induction of human fibroblast MRC5 cells with only four iPS factors (Fig. 1, *C* and *D*). We next performed a parallel experiment using either a WW-domain (binding domain) mutant (W34A) or a peptidyl prolyl isomerase-domain (catalytic domain) mutant (K63A) of Pin1. We confirmed the equivalent expression of each of these mutants and wild-type Pin1 (Fig. 1*E*). Neither of these mutants could boost iPS cell colony formation to the level seen with wild-type Pin1 (Fig. 1*F*), indicating that both the WW and PPIase domains are required for this function.

To test pluripotency *in vivo*, we transplanted 4F plus Pin1-introduced iPS cells subcutaneously into the dorsal flanks of immunodeficient mice. Nine weeks after injection, we observed teratoma formation composed of various tissues including gut-like epithelial tissues (endoderm), striated muscle (mesoderm), cartilage (mesoderm), neural tissues (ectoderm), and epidermal tissues (ectoderm) (Fig. 1*G*). These results indicate that the expression of Pin1 with defined reprogramming factors accelerates the frequency of iPS cell generation.

Pin1 Is Required for Pluripotent Stem Cell Self-renewal and Colony Formation—We next addressed whether Pin1 indeed plays any roles in the self-renewal of human iPS cells. iPS cells were dissociated with accutase and then plated at a clonal density in the presence of several concentrations of the selective Pin1 inhibitor juglone (5-hydroxy-1,4-naphthoquinone) (25, 26). The blockade of Pin1 by juglone considerably reduced both the numbers and size of the colonies in a dose-dependent manner (Fig. 2, *A–C*). It was notable also that the concentration of juglone used did not illicit nonspecific toxic effects in the feeder mouse embryonic fibroblast cells (Fig. 2*A* and data not shown). The effect of Pin1 inhibition upon colony formation was also confirmed in feeder-free cultures of human iPS cells by AP staining (Fig. 2*D*). Moreover, treatment with the Pin1 inhibitory phosphopeptide PINTIDE (27), but not a nonphosphorylated control peptide, significantly reduced the colony formation of human iPS cells (Fig. 2, *E* and *F*).

We next investigated the effects of Pin1 inhibition upon colony formation in murine ES cells. The blockade of Pin1 by juglone significantly reduced the colony numbers in two different murine ES cell types, BDF2 and R1 (Fig. 3*A*). The adenovirus-mediated transduction of a GFP-fused dominant-negative Pin1 (GFP-dnPin1) (28), but not a GFP control, significantly suppressed colony formation in murine ES (R1) cells manifesting as a considerable reduction in both the numbers and colony size of the murine ES cells (Fig. 3, *B–D*). These results together demonstrate that Pin1 is indispensable for the self-renewal and proliferation of pluripotent stem cells.

Pin1 Functions in Maintenance of Pluripotency—We next asked whether Pin1 has any roles in the maintenance of pluripotency in stem cells. Human iPS cells were dissociated and then cultured for 5 days to form colonies. When human iPS cells are cultured in hES medium supplemented with basic fibroblast growth factor, the overwhelming majority of the cells in the colonies are undifferentiated (Fig. 4*A*). However, treatment with juglone resulted in aberrant cell differentiation resulting in a "mosaic pattern" of iPS cell colonies following AP staining (Fig. 4*A*). Similarly, the adenovirus-mediated transduction of GFP-dnPin1, but not a GFP control, prominently reduced the number of AP-positive undifferentiated cells in murine ES cell colonies (Fig. 4*B*). These results together indicate that Pin1 can sustain pluripotent stem cells in an undifferentiated state in addition to the enhancement of self-renewal.

FIGURE 2. **Defective self-renewal of human iPS cells caused by Pin1 inhibition.** *A–C*, human iPS cells were dissociated with accutase and then plated on a feeder cell layer at a clonal density in the presence of the indicated concentrations of juglone for 3 days. Colony formation was analyzed by phase-contrast microscopy (*A*). The number of colonies was counted at 3 days after treatment (*B*). The number of cells per colony was determined by manually counting the DAPI-stained cells (*C*). Data are the mean ± S.E. *D*, human iPS cells were plated at a clonal density on the feeder-free culture in the presence of the indicated concentrations of juglone followed by AP staining. *E* and *F*, human iPS cells were dissociated with accutase and then plated on feeder-free dishes at a clonal density in the presence of 50 μg/ml of the Pin1 inhibitory phosphopeptide PINTIDE (RRRRRRRRRWFYpSPRLKK) or a nonphosphorylated control peptide (RRRRRRRRRWFYAPRLKK) for 48 h (*E*). AP-positive colony numbers were scored (*F*). Data are the mean ± S.E. *Scale bar*, 50 μm.

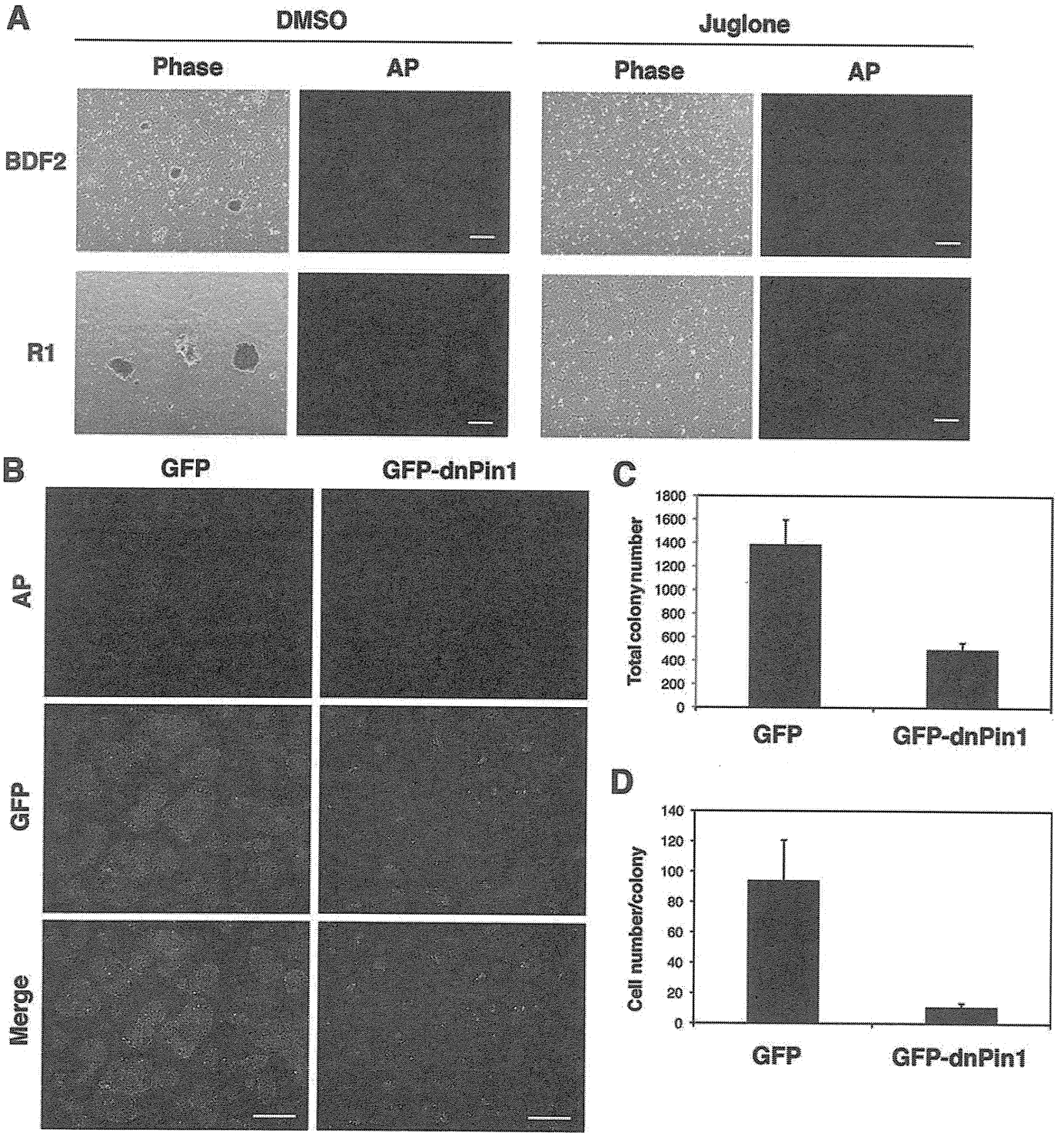

FIGURE 3. **Pin1 inhibition suppresses colony formation in murine ES cells.** *A*, two different murine ES cell types (BDF2 and R1) were plated on gelatin-coated dishes and treated with either DMSO or juglone (10 μM). Colonies were stained with AP (*red*). *Scale bar*, 200 μm. *B–D*, murine ES cells (R1) were infected with an adenovirus vector encoding either GFP or GFP-dnPin1 (3000 viral particles/cell). The cells were then stained with AP (*red*) and DAPI and analyzed by immunofluorescent microscopy (*B*). *Scale bar*, 200 μm. The total colony number (*C*) and the number of cells per colony (*D*) were then determined. Data are the mean ± S.E.

Identification of Pin1 Binding Proteins in Human iPS Cells—Our initial data indicated that Pin1 could enhance the function of reprogramming factors during the induction and maintenance of pluripotency. We next identified the substrates targeted by Pin1 in human iPS cells. Using a monoclonal Pin1 antibody, we co-immunoprecipitated proteins from human iPS cell lysates treated with a phosphatase inhibitor mixture. These isolated immune complexes were then boiled and resolved by one-dimensional SDS-PAGE, and the proteins were visualized using silver staining. Continuous regions of the gel corresponding to proteins of ~30 to 150 kDa in size were systematically excised (Fig. 5*A*), digested with trypsin, and analyzed in a linear

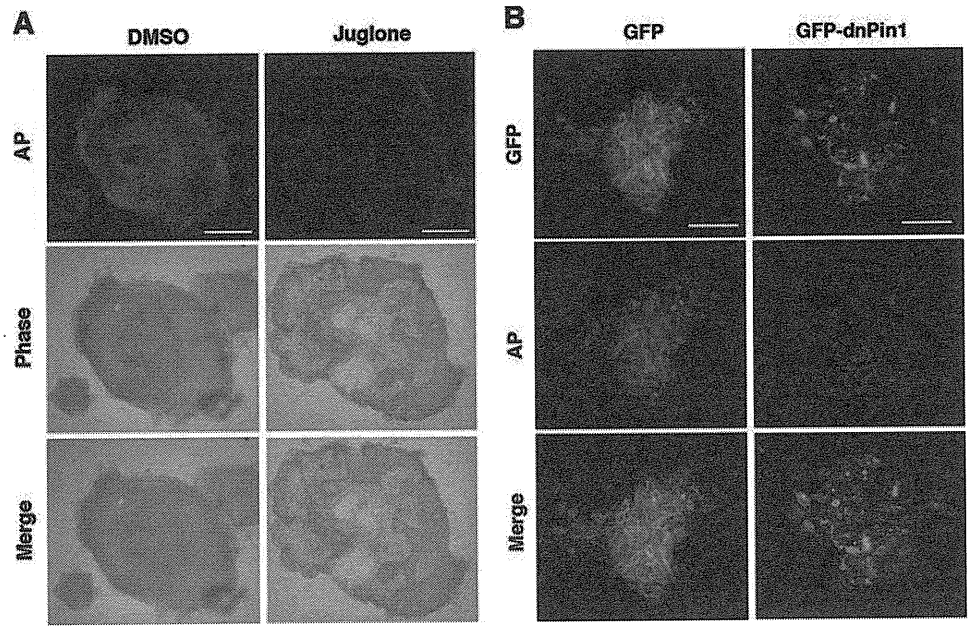

FIGURE 4. **Pin1 inhibition leads to the aberrant cell differentiation of human iPS cells.** *A*, human iPS cells were cultured for 5 days before forming colonies and then treated with either DMSO or juglone (10 μM) for 3 days. The cells were then stained with AP (*red*). Representative images of phase-contrast microscopy and fluorescent immunocytochemistry are shown. *Scale bar*, 200 μm. *B*, mouse ES cells were cultured for 2 days before forming colonies and then infected with an adenovirus vector encoding either GFP or GFP-dnPin1 (3000 viral particles/cell). After 48 h, the cells were then stained with AP (*red*) and DAPI (*blue*) and analyzed by immunofluorescent microscopy. *Scale bar*, 50 μm.

ion trap (LTQ) Orbitrap hybrid mass spectrometer. Peptide mass fingerprinting with the Mascot and Aldente search algorithms subsequently identified 23 Pin1 interacting proteins in human iPS cells (Fig. 5*B*). Notably, these Pin1-binding proteins included the pluripotent transcription factor Oct4. Because Oct4 has been shown to be a master regulator of pluripotency (29), we decided to further analyze the Oct4-Pin1 interaction.

Pin1 Binds and Regulates Protein Stability of Oct4—To further characterize the Oct4-Pin1 interaction, a GST pulldown analysis was initially performed. We found that recombinant GST-Pin1, but not GST alone, binds Oct4. This association was completely abolished by pretreatment of the cell lysates with calf intestine alkaline phosphatase (Fig. 6*A*), indicating that Pin1 binds phosphorylated Oct4. Immunofluorescence analysis further demonstrated that Pin1 co-localizes with Oct4 in the nuclei of iPS cells (Fig. 6*B*). Pin1 has been shown to regulate the stability of its substrate proteins upon binding (17), and we thus addressed whether this was the case for Oct4. Cycloheximide analysis using HeLa cells transfected with Oct4 alone or co-transfected with Oct4 and Pin1 revealed that the protein half-life of Oct4 is significantly enhanced in cells co-expressing Pin1 (Fig. 6*C*). Moreover, immunoprecipitation analysis with cells co-transfected with Oct4 and Myc-tagged ubiquitin, with or without Pin1 co-transfection, further revealed that Pin1 overexpression significantly reduces the polyubiquitination of the Oct4 protein (Fig. 6*D*). Consistently, the Oct4 protein expression level was significantly reduced in human iPS cells treated with juglone as compared with control cells (Fig. 6*E*). These results together confirm that Pin1 enhances the protein stability of Oct4 by suppressing ubiquitin proteasome-mediated proteolysis.

We next investigated the gene expression profile of Oct4 during the inhibition of Pin1. Murine ES cells were transfected with pGL4-Oct4-2601 promoter (harboring a genomic fragment of the Oct4 gene 5′-upstream region) and treated or not with juglone. Pin1 inhibition by juglone did not affect the transcriptional activity of the Oct4 promoter (Fig. 6*F*). Consistently, the results of parallel quantitative RT-PCR analysis demonstrated that the Oct4 mRNA level was not significantly altered by Pin1 inhibition (Fig. 6*G*), whereas the Oct4 protein level was significantly reduced by juglone treatment, as revealed by immunoblot analysis (Fig. 6*H*). These results together indicate that Pin1 regulates the protein stability of Oct4 but not Oct4 transcription.

We next addressed whether Pin1 enhances the transcriptional activity of the Oct4 protein. A luciferase reporter assay using the Oct-Sox enhancer region derived from the FGF4 gene was performed in HeLa cells co-transfected with Oct4, SOX2 or Pin1. Although the sole expression of Pin1 had no significant effects, the co-expression of Oct4 and Pin1 produced a significant increase in reporter activity in a dose-dependent fashion (Fig. 6*I*). This indicated that Pin1 promotes Oct4-mediated transcriptional activation. We performed a parallel experiment using the W34A and K63A Pin1 mutants. Neither of these mutants up-regulated the transcriptional activity of Oct4 to the levels seen with wild-type Pin1 (Fig. 6*J*), indicating that both the WW and PPIase domains are required for this function.

Pin1 Interacts with Ser^{12}-Pro motif of Oct4—To identify the specific Pin1 binding site within the Oct4 protein, we generated several Oct4 deletion mutants and performed GST-pulldown analysis. These experiments revealed that a C-terminal Oct4 deletion mutant (representing amino acids 1–297) could still bind Pin1, but that three extended N-terminal deletion mutants (amino acids 138–360, 113–360, or 34–360) failed to do so (Fig. 7*A*). These data indicate that Pin1 binds to Oct4 in the region between amino acids 1 and 34. Previous reports have indicated

A

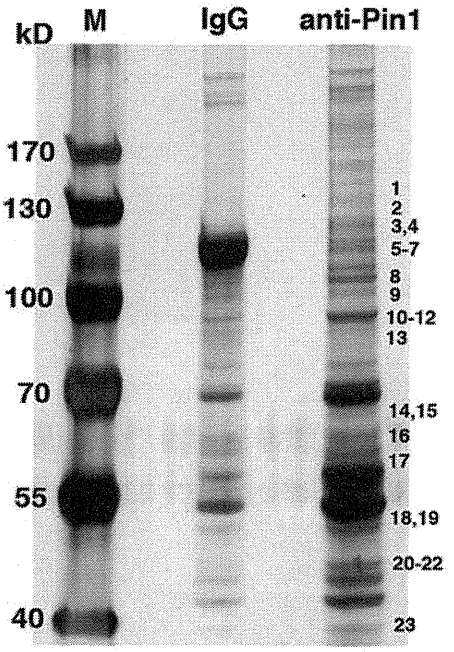

B

No.	Accession No.	Gene description	Predicted size
1	ADCY5_HUMAN	Adenylate cyclase type 5	138818
2	CCD40_HUMAN	Coiled-coil domain-containing protein 40	130033
3	PK3CA_HUMAN	Phosphatidylinositol-4,5-bisphosphate 3-kinase catalytic subunit alpha	124203
4	ZEB1_HUMAN	Zinc finger E-box-binding homeobox 1	123997
5	VINC_HUMAN	Vinculin	123722
6	RADIL_HUMAN	Ras-associating and dilute domain-containing protein	117351
7	UBP2L_HUMAN	Ubiquitin-associated protein 2-like	114465
8	DSG1_HUMAN	Desmoglein-1	113644
9	ENPP3_HUMAN	Ectonucleotide pyrophosphatase/phosphodiesterase family member 3	100059
10	ZN337_HUMAN	Zinc finger protein 337	86819
11	NASP_HUMAN	Nuclear autoantigenic sperm protein	85186
12	ZY11B_HUMAN	Protein zyg-11 homolog B	83921
13	MPEG1_HUMAN	Macrophage-expressed gene 1 protein	78587
14	FA13C_HUMAN	Protein FAM13C	65687
15	VPS45_HUMAN	Vacuolar protein sorting-associated protein 45	65036
16	ANR53_HUMAN	Ankyrin repeat domain-containing protein 53	59493
17	RPA34_HUMAN	DNA-directed RNA polymerase I subunit RPA34	54951
18	VIME_HUMAN	Vimentin	53619
19	KCAB1_HUMAN	Voltage-gated potassium channel subunit beta-1	46534
20	PRS8_HUMAN	26S protease regulatory subunit 8	45597
21	FKBP8_HUMAN	Peptidyl-prolyl cis-trans isomerase FKBP8	44534
22	PO5F1_HUMAN	POU domain, class 5, transcription factor 1 (OCT4)	38571
23	THAP1_HUMAN	THAP domain-containing protein 1	24928

FIGURE 5. **Identification of Pin1-binding proteins in human iPS cells.** *A* and *B*, lysates of human iPS cells were subjected to immunoprecipitation with either non-immunized control mouse IgG (IgG) or mouse anti-Pin1 monoclonal antibodies. Proteins bound to protein A/G-agarose beads were isolated, resolved by SDS-PAGE, and detected by silver staining (*A*). *M* indicates protein marker. Excised gel bands were digested with trypsin and analyzed on a linear ion trap (LTQ) Orbitrap hybrid mass spectrometer followed by peptide mass fingerprinting with the Mascot and Aldente search algorithms (*B*).

that Pin1 can bind only phosphorylated Ser/Thr-Pro motifs (17, 27) of which only one (Ser^{12}-Pro) exists between residues 1 and 34 in the Oct4 protein. Interestingly, this motif is conserved between various species including human, mouse, rat, and rabbit (Fig. 7*B*). We generated an Oct4 site-directed mutant at this site by substituting serine 12 for alanine (S12A). GST pulldown analysis subsequently revealed that Pin1 binds wild-type Oct4, but not its S12A mutant (Fig. 7*C*). These results confirm that Pin1 indeed bind the phosphorylated Ser^{12}-Pro motif of Oct4.

To further examine the functional interactions between Pin1 and Oct4 on this site, we next investigated the nature of the S12A mutant in terms of its protein expression in the presence of Pin1. HeLa cells were transfected with either wild-type Oct4 or its S12A mutant and co-transfected with Pin1. This was followed by immunoblotting analysis. We found that Pin1 increased the expression levels of wild-type Oct4, but not the S12A mutant (Fig. 7*D*).

DISCUSSION

In our present study, we report that Pin1 is an essential regulator of the self-renewal and maintenance of pluripotent stem cells. We further found the following: 1) Pin1 is induced upon the induction of human iPS cells; 2) the co-expression of Pin1 with defined reprogramming factors significantly enhances the

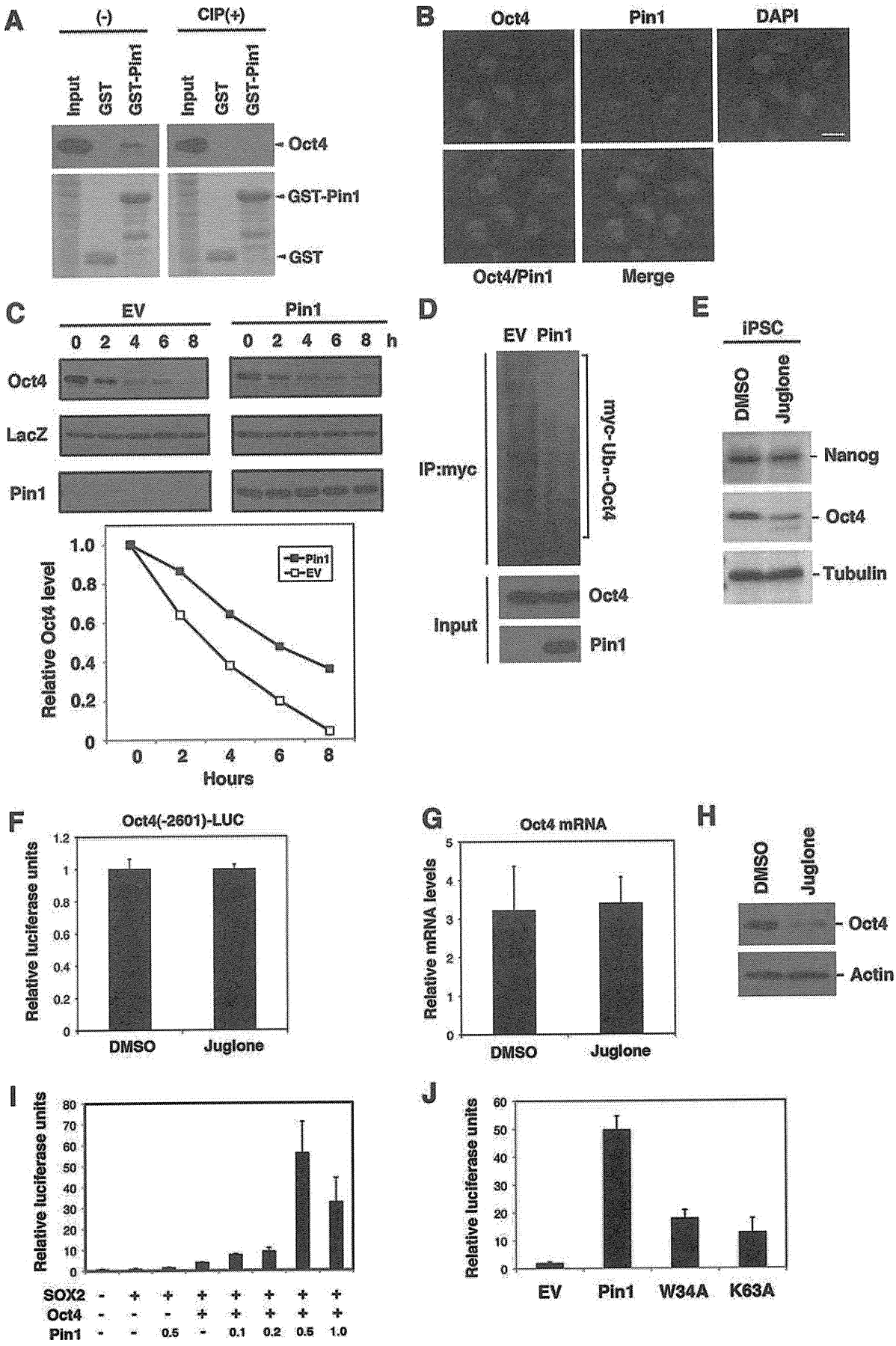
A
(-)
CIP(+)
Input
GST
GST-Pin1
Oct4
GST-Pin1
GST
B
Oct4
Pin1
DAPI
Oct4/Pin1
Merge
C
EV
Pin1
0 2 4 6 8
0 2 4 6 8 h
Oct4
LacZ
Pin1
Relative Oct4 level
Pin1
EV
Hours
D
EV Pin1
IP:myc
myc-Ub$_n$-Oct4
Input
Oct4
Pin1
E
iPSC
DMSO
Juglone
Nanog
Oct4
Tubulin
F
Oct4(-2601)-LUC
Relative luciferase units
DMSO
Juglone
G
Oct4 mRNA
Relative mRNA levels
DMSO
Juglone
H
DMSO
Juglone
Oct4
Actin
I
Relative luciferase units
SOX2
Oct4
Pin1
0.5
0.1
0.2
0.5
1.0
J
Relative luciferase units
EV
Pin1
W34A
K63A

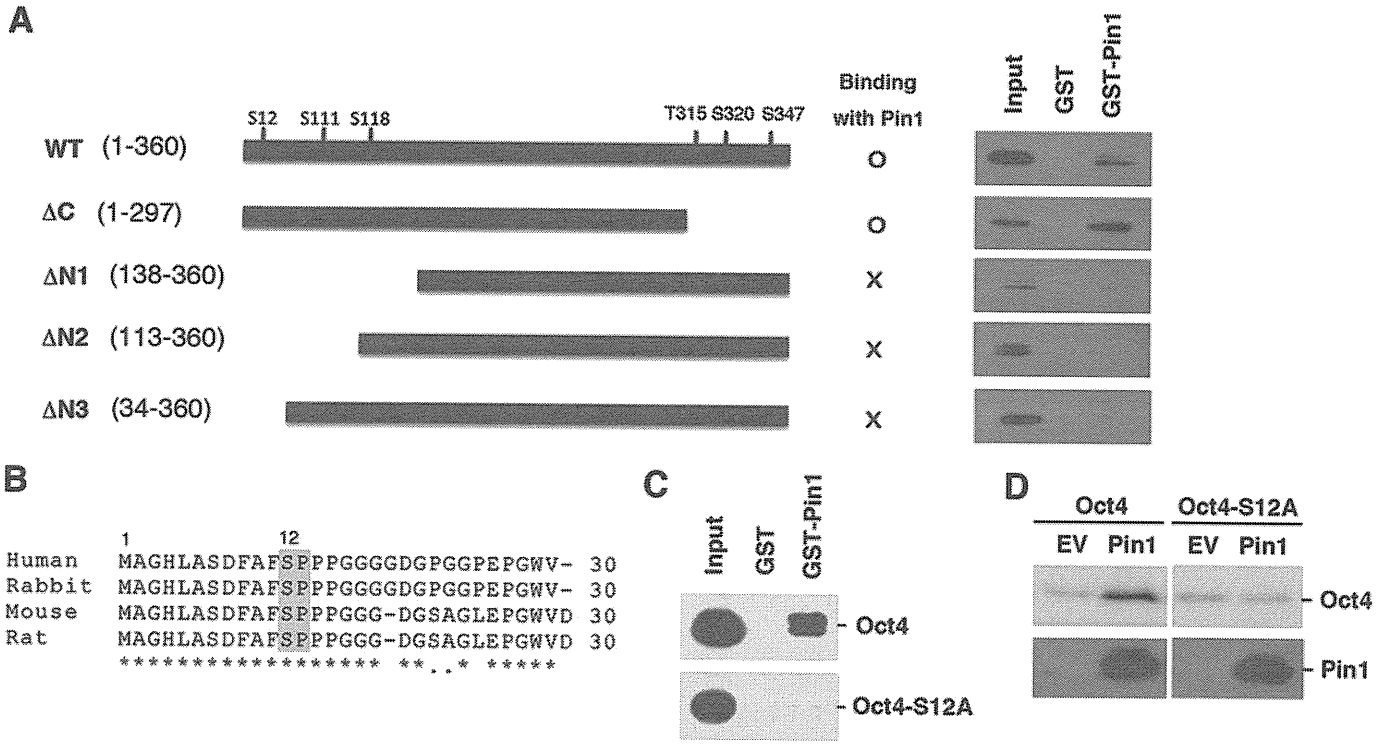

FIGURE 7. **Pin1 interacts with the Ser[12]-Pro motif of Oct4.** *A*, schematic representation of the Oct4 deletion mutants generated in this study (*left panel*). HeLa cells were transfected with the indicated Oct4 deletion mutants for 24 h. Cell lysates were then prepared and subjected to GST pulldown analysis with either GST or GST-Pin1 followed by immunoblotting analysis with Oct4 antibodies (*right panel*). *B*, amino acid sequence alignment of the human, rabbit, mouse, and rat Oct4 proteins. The conserved Ser[12]-Pro motifs are *boxed*. *C*, HeLa cells were transfected with the Oct4 site-directed mutant Oct4-S12A and subjected to GST pulldown analysis. *D*, HeLa cells were transfected with wild-type Oct4 or its S12A mutant with or without Pin1. After 24 h, the cells were subjected to immunoblotting analysis with an anti-Oct4 antibody.

frequency of iPS cell induction; 3) the blockade of Pin1 significantly inhibits the colony formation of dissociated human iPS cells and murine ES cells; 4) Pin1 inhibition leads to the aberrant cell differentiation in human iPS cells and murine ES cells after forming colonies; 5) Oct4 is a putative Pin1 substrate in human iPS cells; and 6) Pin1 interacts with Oct4 at its Ser[12]-Pro motif and facilitates its stability and enhanced transcriptional activity. Our findings thus uncover a novel role of Pin1 as a putative regulator of the self-renewal and survival of pluripotent stem cells via Oct4 function.

Our current results add to previous findings indicating that Pin1 is a multifunctional protein that mediates various phosphorylated proteins involved in divergent cellular processes (17). This implicates Pin1 as a modulator of multiple signaling pathways depending on the cell type and biological context. Indeed, we demonstrate in our present study that Pin1 is a crucial regulator of the phosphorylation-dependent intracellular signaling network that controls cellular stemness and pluripotency. Moreover, iPS cells induced by the expression of four Yamanaka factors (Oct4, SOX2, Klf4, and c-Myc) led to a high expression level of Pin1, and these cells were found to be dependent on Pin1 function. This suggests that Pin1 could be one of the crucial factors in the induction of iPS cells from somatic cells that functions by cooperating with reprogramming transcription factors.

FIGURE 6. **Pin1 interacts with phosphorylated Oct4 and enhances its transcriptional activity.** *A*, human iPS cell lysates treated or untreated with calf intestine alkaline phosphatase were subjected to GST pulldown analysis with either GST or GST-Pin1, followed by immunoblotting analysis with anti-Oct4 antibody (*upper panel*). Coomassie staining for the GST or GST-Pin1 used in the assay is shown in the *lower panel*. *B*, human iPS cells were fixed with 4% paraformaldehyde and then co-immunostained with monoclonal antibodies against Oct4 (*green*) and polyclonal antibodies against Pin1 (*red*). Cells were then analyzed by confocal microscopy. *Scale bar*, 10 μm. *C*, HeLa cells transfected with the indicated vectors and HA-LacZ cells were treated with cycloheximide and harvested at the indicated time points. This was followed by immunoblotting analysis with Oct4, Pin1, and HA antibodies (*upper panel*). Quantitative data are shown in the *lower panel*. *D*, HeLa cells were transfected with Myc-tagged ubiquitin, Oct4, and co-transfected with either empty vector (*EV*) or Pin1. Cells were then treated with MG-132 for 12 h, and lysates were prepared and immunoprecipitated with anti-Myc antibody followed by immunoblotting analysis with anti-Oct4 antibody. Total cell lysates prior to immunoprecipitation (input) were immunoblotted with anti-Pin1 or anti-Oct4 antibody. *E*, human iPS cells were plated on Matrigel-coated feeder-free dishes and treated with either DMSO or juglone (20 μM) for 24 h. Cell lysates were then processed for immunoblotting analysis with anti-Nanog, anti-Oct4, or anti-tubulin antibodies. *F*, a plasmid containing the luciferase (*LUC*) gene flanked with 2601 bp of the Oct4 5′-upstream region was transfected into murine ES cells. The resulting cells were cultured in Matrigel-coated feeder-free dishes and treated with either DMSO or juglone (10 μM) for 24 h, and analyzed by gene reporter assay. *G*, murine ES cells were cultured in Matrigel-coated feeder-free dishes and treated with either DMSO or juglone (10 μM) for 24 h. Total RNAs were then extracted and reverse-transcribed. These preparations were then subjected to quantitative RT-PCR analysis for Oct4. The transcript levels were normalized using GAPDH. *H*, murine ES cells were cultured in Matrigel-coated feeder-free dishes and treated with either DMSO or juglone (10 μM) for 24 h. Cell lysates were then processed for immunoblotting analysis with either anti-Oct4 or anti-β-actin antibody. *I*, HeLa cells were transiently transfected with plasmids encoding Oct4, SOX2, or Pin1 and co-transfected with Oct-SOX reporter gene and pRL-CMV. At 24 h post-transfection, the cells were collected and subjected to a gene reporter assay. *J*, HeLa cells were transiently transfected with an Oct-SOX reporter gene and co-transfected with plasmids encoding wild-type Pin1 or its W34A or K63A mutants, together with Oct4 and SOX2. At 24 h post-transfection, the cells were collected and subjected to a gene reporter assay.

The molecular mechanisms underlying the regulation of Pin1 in the induction and maintenance of pluripotency are likely to be highly complex given that Pin1 interacts with multiple substrates in pluripotent stem cells, as revealed by our proteomics analysis. However, our current findings also indicate that Pin1 is involved in the growth and maintenance of pluripotency in stem cells through its phosphorylation-dependent prolyl isomerization of substrates such as Oct4. In this regard, a recent report by Moretto-Zita *et al.* (30) has demonstrated that Pin1 can also associate with another pluripotent transcription factor, Nanog, in murine ES cells and sustain the self-renewal and teratoma formation of these cells in immunodeficient mice. These results indicate that Pin1 is a crucial modulator of the transcription factor network governing cellular stemness. It is possible also that Pin1 could regulate this process by modulating the function of other substrates. Further studies of Pin1 function in stem cells at various stages might shed new light on the underlying molecular pathways and factors that control self-renewal and multipotency.

It has been demonstrated that Pin1 knock-out mice develop normally but display some proliferation abnormalities, including a decreased body weight, retinal degeneration, and impaired mammary gland development (31, 32). Pin1 knock-out mice also exhibit testicular atrophy with a significantly impaired proliferation of primordial germ cells and the progressive loss of spermatogenic cells (33). These phenotypes can now be attributed to the impaired maintenance and proliferation of germ-related stem cells due to the loss of Pin1 function.

In many circumstances, Pin1 acts as either a repressor or an enhancer of the degradation of substrate proteins (15–17, 34). Our current data now additionally demonstrate that Pin1 can also prolong the protein half-life of Oct4, thereby enhancing its transcriptional activity. Oct4 has been shown to be regulated by post-translational modifications such as SUMOlylation (35). Our current findings reveal that Oct4 is also regulated by phosphorylation and subsequent prolyl isomerization. Identification of the kinase(s) responsible for the association of Pin1 and Oct4 will enhance our understanding of the regulatory pathways that operate during and after the induction of pluripotency.

It is desirable to utilize pluripotent stem cells such as iPS cells for future regenerative medicine applications. However, there are already concerns surrounding the use of iPS cells in a clinical setting because prior studies have suggested that they are likely to develop cancers (4, 36). Our current findings suggest, however, that the Pin1 inhibition could effectively block the proliferation of iPS cells in an undifferentiated state. Pin1 could therefore act as a molecular switch that can reversibly control the proliferation and survival of iPS cells, thereby reducing the risk of cell transformation and tumor formation.

Acknowledgments—We are grateful to the Riken Bioresource Center for providing human iPS cells and MRC5 fibroblasts. We also thank M. Machida, A. Hosoda, and S. Yoshizaki for comments on the manuscript and critical discussions and S. Baba and T. Taniguchi for technical assistance.

REFERENCES

1. Thomson, J. A., Itskovitz-Eldor, J., Shapiro, S. S., Waknitz, M. A., Swiergiel, J. J., Marshall, V. S., and Jones, J. M. (1998) *Science* **282,** 1145–1147
2. Watt, F. M., and Hogan, B. L. (2000) *Science* **287,** 1427–1430
3. Lewitzky, M., and Yamanaka, S. (2007) *Curr. Opin. Biotechnol.* **18,** 467–473
4. Takahashi, K., and Yamanaka, S. (2006) *Cell* **126,** 663–676
5. Boyer, L. A., Lee, T. I., Cole, M. F., Johnstone, S. E., Levine, S. S., Zucker, J. P., Guenther, M. G., Kumar, R. M., Murray, H. L., Jenner, R. G., Gifford, D. K., Melton, D. A., Jaenisch, R., and Young, R. A. (2005) *Cell* **122,** 947–956
6. Eiselleova, L., Matulka, K., Kriz, V., Kunova, M., Schmidtova, Z., Neradil, J., Tichy, B., Dvorakova, D., Pospisilova, S., Hampl, A., and Dvorak, P. (2009) *Stem Cells* **27,** 1847–1857
7. Dvorak, P., Dvorakova, D., Koskova, S., Vodinska, M., Najvirtova, M., Krekac, D., and Hampl, A. (2005) *Stem Cells* **23,** 1200–1211
8. Li, J., Wang, G., Wang, C., Zhao, Y., Zhang, H., Tan, Z., Song, Z., Ding, M., and Deng, H. (2007) *Differentiation* **75,** 299–307
9. Sun, H., and Tonks, N. K. (1994) *Trends Biochem. Sci.* **19,** 480–485
10. Brill, L. M., Xiong, W., Lee, K. B., Ficarro, S. B., Crain, A., Xu, Y., Terskikh, A., Snyder, E. Y., and Ding, S. (2009) *Cell Stem Cell* **5,** 204–213
11. Prudhomme, W., Daley, G. Q., Zandstra, P., and Lauffenburger, D. A. (2004) *Proc. Natl. Acad. Sci. U.S.A.* **101,** 2900–2905
12. Hunter, T. (2009) *Curr. Opin. Cell Biol.* **21,** 140–146
13. Lu, K. P., Hanes, S. D., and Hunter, T. (1996) *Nature* **380,** 544–547
14. Ryo, A., Liou, Y. C., Lu, K. P., and Wulf, G. (2003) *J. Cell Sci.* **116,** 773–783
15. Ryo, A., Suizu, F., Yoshida, Y., Perrem, K., Liou, Y. C., Wulf, G., Rottapel, R., Yamaoka, S., and Lu, K. P. (2003) *Mol. Cell* **12,** 1413–1426
16. Ryo, A., Nakamura, M., Wulf, G., Liou, Y. C., and Lu, K. P. (2001) *Nat. Cell Biol.* **3,** 793–801
17. Lu, K. P., and Zhou, X. Z. (2007) *Nat. Rev. Mol. Cell Biol.* **8,** 904–916
18. Esnault, S., Shen, Z. J., and Malter, J. S. (2008) *Crit. Rev. Immunol.* **28,** 45–60
19. Takahashi, K., Okita, K., Nakagawa, M., and Yamanaka, S. (2007) *Nat. Protoc.* **2,** 3081–3089
20. Yamada, M., Hamatani, T., Akutsu, H., Chikazawa, N., Kuji, N., Yoshimura, Y., and Umezawa, A. (2010) *Hum. Mol. Genet.* **19,** 480–493
21. Liu, Y., and Labosky, P. A. (2008) *Stem Cells* **26,** 2475–2484
22. Masui, S., Nakatake, Y., Toyooka, Y., Shimosato, D., Yagi, R., Takahashi, K., Okochi, H., Okuda, A., Matoba, R., Sharov, A. A., Ko, M. S., and Niwa, H. (2007) *Nat. Cell Biol.* **9,** 625–635
23. Yang, H. M., Do, H. J., Oh, J. H., Kim, J. H., Choi, S. Y., Cha, K. Y., Chung, H. M., and Kim, J. H. (2005) *J. Cell. Biochem.* **96,** 821–830
24. Takahashi, K., Ichisaka, T., and Yamanaka, S. (2006) *Methods Mol. Biol.* **329,** 449–458
25. Hennig, L., Christner, C., Kipping, M., Schelbert, B., Rücknagel, K. P., Grabley, S., Küllertz, G., and Fischer, G. (1998) *Biochemistry* **37,** 5953–5960
26. Shen, Z. J., Esnault, S., Schinzel, A., Borner, C., and Malter, J. S. (2009) *Nat. Immunol.* **10,** 257–265
27. Yaffe, M. B., Schutkowski, M., Shen, M., Zhou, X. Z., Stukenberg, P. T., Rahfeld, J. U., Xu, J., Kuang, J., Kirschner, M. W., Fischer, G., Cantley, L. C., and Lu, K. P. (1997) *Science* **278,** 1957–1960
28. Lu, P. J., Zhou, X. Z., Liou, Y. C., Noel, J. P., and Lu, K. P. (2002) *J. Biol. Chem.* **277,** 2381–2384
29. Niwa, H., Miyazaki, J., and Smith, A. G. (2000) *Nat. Genet.* **24,** 372–376
30. Moretto-Zita, M., Jin, H., Shen, Z., Zhao, T., Briggs, S. P., and Xu, Y. (2010) *Proc. Natl. Acad. Sci. U.S.A.* **107,** 13312–13317
31. Fujimori, F., Takahashi, K., Uchida, C., and Uchida, T. (1999) *Biochem. Biophys. Res. Commun.* **265,** 658–663
32. Liou, Y. C., Ryo, A., Huang, H. K., Lu, P. J., Bronson, R., Fujimori, F., Uchida, T., Hunter, T., and Lu, K. P. (2002) *Proc. Natl. Acad. Sci. U.S.A.* **99,** 1335–1340
33. Atchison, F. W., and Means, A. R. (2003) *Biol. Reprod.* **69,** 1989–1997
34. Ryo, A., Hirai, A., Nishi, M., Liou, Y. C., Perrem, K., Lin, S. C., Hirano, H., Lee, S. W., and Aoki, I. (2007) *J. Biol. Chem.* **282,** 36671–36681
35. Zhang, Z., Liao, B., Xu, M., and Jin, Y. (2007) *FASEB J.* **21,** 3042–3051
36. Knoepfler, P. S. (2009) *Stem Cells* **27,** 1050–1056

Tanaka et al. BMC Infectious Diseases 2011, 11:71
http://www.biomedcentral.com/1471-2334/11/71

BMC Infectious Diseases

RESEARCH ARTICLE Open Access

Identification of tuberculosis-associated proteins in whole blood supernatant

Takahiro Tanaka[1,2], Shinsaku Sakurada[2], Keiko Kano[3], Eri Takahashi[3,5], Kazuki Yasuda[4], Hisashi Hirano[5], Yasushi Kaburagi[3], Nobuyuki Kobayashi[6], Nguyen Thi Le Hang[7], Luu Thi Lien[8], Ikumi Matsushita[2], Minako Hijikata[2], Takafumi Uchida[1] and Naoto Keicho[2*]

Abstract

Background: Biological parameters are useful tools for understanding and monitoring complicated disease processes. In this study, we attempted to identify proteins associated with active pulmonary tuberculosis (TB) using a proteomic approach.

Methods: To assess TB-associated changes in the composition of human proteins, whole blood supernatants were collected from patients with active TB and healthy control subjects. Two-dimensional difference gel electrophoresis (2D-DIGE) was performed to analyze proteins with high molecular weights (approximately >20 kDa). Baseline protein levels were initially compared between patients with active TB and control subjects. Possible changes of protein patterns in active TB were also compared *ex vivo* between whole blood samples incubated with *Mycobacterium tuberculosis* (*Mtb*)-specific antigens (stimulated condition) and under unstimulated conditions. Immunoblot and enzyme-linked immunosorbent assays (ELISA) were performed to confirm differences in identified proteins.

Results: Under the baseline condition, we found that the levels of retinol-binding protein 4 (RBP4), fetuin-A (also called α-HS-glycoprotein), and vitamin D-binding protein differed between patients with active TB and control subjects on 2D gels. Immunoblotting results confirmed differential expression of RBP4 and fetuin-A. ELISA results further confirmed significantly lower levels of these two proteins in samples from patients with active TB than in control subjects ($P < 0.0001$). *Mtb*-specific antigen stimulation *ex vivo* altered clusterin expression in whole blood samples collected from patients with active TB.

Conclusions: We identified TB-associated proteins in whole blood supernatants. The dynamics of protein expression during disease progression may improve our understanding of the pathogenesis of TB.

Background

Tuberculosis (TB) is one of the most important infectious causes of death worldwide [1]. Despite its long historical interaction with humans, our understanding of host response to the TB pathogen remains incomplete. Investigation of the molecular basis of differences in the host immune status and metabolism between patients with active TB and control subjects may provide a clue to understand the disease process, and thus contribute to future strategies for TB prevention and treatment.

Recent advances in comprehensive analytical techniques, such as transcriptomics and proteomics, have enabled us to identify proteins associated with active TB in humans. As a pioneering approach, Jacobsen et al. compared the gene expression profiles of peripheral blood mononuclear cells from patients with TB and *Mtb*-infected healthy donors by microarray analysis [2], and Mistry et al. analyzed gene expression patterns in whole blood in an attempt to find a candidate biomarker for discriminating cured patients from those with a risk of relapse [3].

Agranoff et al. [4] identified amyloid A and transthyretin in human serum as potential indicators for distinguishing patients with TB from those with non-TB

* Correspondence: nkeicho-tky@umin.ac.jp
[2]Department of Respiratory Diseases, Research Institute, National Center for Global Health and Medicine, 1-21-1 Toyama, Shinjuku-ku, Tokyo 162-8655, Japan
Full list of author information is available at the end of the article

inflammatory conditions. They also reported that a combination of four protein markers, including amyloid A and transthyretin, achieved a diagnostic accuracy of up to 78%. Chegou et al. [5] reported that EGF, VEGF, TGF-α, and sCD40L in supernatants obtained from interferon-gamma (IFN-γ)-release assays (IGRAs) are informative markers for differentiating active disease from latent infection. Although the above studies are promising, such comprehensive analytical techniques are still in the developmental stages and further investigations are required before they can be applied clinically.

IGRA detects TB infection by measuring the *Mtb*-specific immune response with high specificity [6]. IFN-γ is released by reactivation of *Mtb*-specific effector memory T cells in whole blood. Despite its advantages, IGRA is not a perfect tool for use in most developing countries. In countries with a high TB burden, patients with active TB, and not those with latent TB infection, need to be immediately identified and treated in order to prevent disease transmission. However, IGRA is not capable of distinguishing active TB from latent infection. Also, cytokine measurements to be performed for IGRA are rather expensive in a resource-limited setting and difficult to distribute. Thus, from a practical as well as a research standpoint, development of new markers for TB is desired.

In the present study, by high-resolution two-dimensional difference gel electrophoresis (2D-DIGE) followed by liquid chromatography-mass spectrometry (LC-MS), we analyzed the expression profiles of high molecular weight proteins (approximately >20 kDa) that have not been studied fully among components of residual whole blood supernatants after performing IGRA.

We used two comparative frameworks. One was the direct comparison of plasma supernatants collected from patients with active TB and healthy control subjects. This comparison aimed to identify proteins that are markedly upregulated or downregulated in the disease state; even if such proteins are not disease specific, they might act as useful markers for monitoring the disease before, during, and after treatment. The other comparative framework was more TB specific since whole blood samples from patients were stimulated with *Mtb*-specific antigens or left unstimulated, and the results were compared.

Methods

Patients and control subjects

In this study, whole blood samples collected from Japanese and Vietnamese individuals were used. The study was approved by the ethical review committees of the National Center for Global Health and Medicine (formerly the International Medical Center of Japan), Tokyo, Japan, and the Ministry of Health, Vietnam. Written informed consent was obtained from each participant. Blood samples were collected from patients with active TB immediately before (Vietnamese patient samples) or within 7 days (Japanese patient samples) of treatment initiation. Patients with potential complications attributable to malignancies, autoimmune diseases, or HIV coinfection were excluded from the study.

At the initial screening and confirmation stage, blood samples were collected from 14 Japanese patients with bacteriologically confirmed active pulmonary TB (9 men and 5 women; median age 50 years, range 22-75 years) and 13 age- and gender-matched healthy Japanese patients (8 men and 5 women; median age 48 years, range 24-64 years). We could not completely rule out the possibility of latent TB infection in 2 of the 13 control subjects, according to the results of a commercially available IGRA (QuantiFERON®-TB Gold in Tube; Cellestis, Victoria, Australia). However, we analyzed all samples together at the initial stage to identify proteins associated with active TB disease. The tuberculin skin test was not useful for detecting latent TB infection in our study since most individuals in the tested populations had received BCG vaccination after birth. Blood samples from 4 patients with active TB and 4 healthy individuals were chosen for screening by 2D-DIGE and immunoblotting. The stability of proteins measured by the enzyme-linked immunosorbent assay (ELISA) was investigated by comparing a set of plasma samples directly separated from EDTA-containing peripheral blood and another set of plasma supernatants obtained from heparinized blood after 18 h of incubation (under the same conditions as the IGRA negative control).

At the next verification stage, we utilized samples from 25 Vietnamese patients with sputum smear-positive active pulmonary TB (13 men and 12 women; median age 35 years, range 20-55 years) and 50 age- and gender-matched Vietnamese healthy control subjects (26 men and 24 women; median age 36 years, range 21-54 years) of which 25 were IGRA positive and 25 were IGRA negative. None of the IGRA-positive individuals had any signs or symptoms of active TB but at least some were reasonably suspected to have latent TB infections because the prevalence of TB in the population is high. Following IGRA, the remaining unstimulated plasma supernatants were used for ELISA.

Sample collection and preparation

Whole blood was separately collected in heparin-containing tubes precoated with mitogen as a positive control or cocktails of ESAT-6, CFP-10, and TB7.7 (p4) peptides as *Mtb*-specific antigens (QuantiFERON®-TB Gold in Tube; Cellestis); the negative control tubes had no precoat. After 18 h of incubation at 37°C, each sample was centrifuged and the plasma supernatants were

harvested and stored at -80°C until use in subsequent assays. For proteomic analysis, four sample sets that were either unstimulated or stimulated with *Mtb*-specific antigens or mitogen from patients with active pulmonary TB and four corresponding sets from control subjects were used to screen for candidate proteins by 2D-DIGE. To increase resolution, 14 human major plasma proteins (albumin, IgG, antitrypsin, IgA, transferrin, haptoglobin, fibrinogen, alpha 2-macroglobulin, alpha 1-acid glycoprotein, IgM, apolipoprotein Al, apolipoprotein All, complement C3, and transthyretin) were removed prior to electrophoresis using a Multiple Affinity Removal LC Column-Human 14 (Agilent Technologies, Santa Clara, CA, USA). The samples were then concentrated by ultrafiltration (Agilent Technologies, Concentrators Spin 5 kDa MWCO, 4 ml) followed by acetone precipitation in preparation for subsequent electrophoresis.

Quantitative analyses by 2D-DIGE

Protein samples were labeled with Cy3 and Cy5 (DIGE Fluors Minimal Labeling Dyes; GE Healthcare, Buckinghamshire, UK) according to the manufacturer's instructions. The samples (50 μg of total protein per gel) were applied to Immobiline DryStrips (18 cm long, pH 4-7 linear; Amersham Biosciences, Pittsburgh, PA, USA), and isoelectric focusing (IEF) was performed using an Ettan IPGphor IEF system (Amersham Biosciences) according to the manufacturer's instructions. Next, SDS-PAGE was performed using a 10-18% linear gradient gel from DRC Co., Ltd. (Tokyo, Japan). The fluorescence intensity of each protein spot was digitally recorded using a Molecular Imager FX system (Bio-Rad Laboratories, Hercules, CA, USA) with Quantity One software (Bio-Rad Laboratories), and differential protein expression was quantitatively analyzed using the PDQuest software (Bio-Rad Laboratories). The same gel included a reference sample that had been labeled with Cy2 and was used for spot matching, image analysis, and volume normalization. Initially, all spots were roughly matched using an automated tool in the PDQuest software suite. This estimate was followed by a more detailed manual curation to correct any inappropriately matched pairs of protein spots.

Sample preparation for mass spectrometry

A mixture of all samples (400 μg of total protein per gel) was subjected to 2D-DIGE under the same conditions as described above to isolate selected spots. To visualize individual protein spots, the gels were stained with SYPRO Ruby protein gel stain (Molecular Probes, Eugene, OR, USA) for 3 h. The fluorescence intensity of each protein spot was digitally measured using the Molecular Imager FX system with Quantity One software. Mass spectrometric analysis was performed according to the method reported by Toda *et al.* [7], with slight modification. Briefly, each protein spot on SYPRO Ruby stained gels was picked using a spot picker (Amersham Biosciences). In-gel digestion of proteins was performed according to the method reported by Saeki *et al.* [8].

Mass spectrometric analysis

An ESI ion-trap mass spectrometer (LCQ Deca XP Plus, Thermo Electron) was used for peptide detection. Mass spectrometric analysis was performed as described previously [8]. Protein identification was performed using the Mascot server (Matrix Science, Boston, MA, USA) and Protein Prospector (UCSF Mass Spectrometry Facility, San Francisco, CA, USA). We selected the SWISS-PROT *Homo sapiens* database and used the following parameters: peptide tolerance 1.0 Da and one missed cleavage. Carbamidomethyl modification of cysteine, acetylation of the NH2-terminal ends of lysine, and phosphorylation of serine, threonine, or tyrosine were considered in this analysis.

Immunoblotting

Immunoblotting to detect the proteins identified as described above was performed using anti-human retinol-binding protein 4 (RBP4) rabbit polyclonal IgG (A-0040; Dako; Glostrup, Denmark), anti-human fetuin-A (AHSG) goat polyclonal IgG (G-20; Santa Cruz Biotechnology; Santa Cruz, CA, USA), anti-human vitamin D-binding protein (VDBP) (Gc-Globulin) rabbit polyclonal IgG (Dako), anti-human clusterin-α mouse monoclonal IgG1 (B-5; Santa Cruz Biotechnology), or anti-human clusterin-β rabbit polyclonal IgG (N-18; Santa Cruz Biotechnology).

Total protein concentrations were determined using the Bio-Rad protein assay kit (Bio-Rad Laboratories). To detect clusterin-α and -β, mixed protein samples (20 μg) were applied to 2D PAGE with 1D IEF using the Immobiline DryStrip (pH 3-5.6 nonlinear). Proteins were then transferred to PVDF membranes. The membranes were probed with polyclonal antibodies, anti-clusterin-α, and anti-clusterin-β. To detect other proteins, each sample (10 μg) was subjected to conventional SDS-PAGE. Membranes were probed with anti-VDBP, anti-fetuin-A, or anti-RBP4 polyclonal antibodies. Anti-mouse and anti-rabbit (GE Healthcare) as well as anti-goat (Santa Cruz Biotechnology) HRP-conjugated secondary antibodies were prepared. Protein bands were detected using the ECL plus detection reagent (GE Healthcare). Band intensities were calculated using the Quantity One software.